

**GENERAL GEOLOGY OF THE CARBONATE WITHIN A
QUARRY IN NORTHERN PART OF SUNGAI SIPUT, PERAK
WITH AN EMPHASIS ON DOLOMITIZATION**

AIMAN FITRI BIN ZAINAL ABIDIN

PETROLEUM GEOSCIENCE

UNIVERSITI TEKNOLOGI PETRONAS

MAY 2014

AIMAN FITRI BIN ZAINAL ABIDIN B. TECH. (HONS) PETROLEUM GEOSCIENCE

MAY 2014

**General Geology of the Carbonate within a quarry in northern part of Sungai
Siput, Perak with an emphasis on Dolomitization**

By

Aiman Fitri Bin Zainal Abidin

13641

A project dissertation submitted to the Petroleum Geoscience
Department Universiti Teknologi PETRONAS
in partial fulfilment of the requirements for the
BACHELOR OF TECHNOLOGY (HONS)
(PETROLEUM GEOSCIENCE)

MAY 2014

Universiti Teknologi PETRONAS
Bandar Seri Iskandar
31750 Tronoh
Perak Darul Ridzuan

CERTIFICATION OF APPROVAL

**General Geology of the Carbonate within a quarry in northern part of Sungai
Siput, Perak with an emphasis on Dolomitization**

By

Aiman Fitri Bin Zainal Abidin

13641

A project dissertation submitted to the Petroleum Geoscience
Department Universiti Teknologi PETRONAS
in partial fulfilment of the requirements for the
BACHELOR OF TECHNOLOGY (HONS)
(PETROLEUM GEOSCIENCE)

Approved by,

.....

(Dr. Eswaran Padmanabhan)

UNIVERSITI TEKNOLOGI PETRONAS

TRONOH

May 2014

CERTIFICATION OF ORIGINALITY

This is to certify that I am responsible for the work submitted in this project, that the original work is my own except as specified in the references and acknowledgements, and that the original work contained herein have not been undertaken or done by unspecified sources or persons.

.....
AIMAN FITRI BIN ZAINAL ABIDIN

ABSTRACT

Kinta Valley was a main producer of tin-ore in the world around 1876 to 1950. The crystalline limestone is one of the sedimentary rocks here. Mostly of them is been quarried for magnesium oxide, marble and construction materials for the needs of industry domestically or internationally. The limestone here became the interest of people due to its potential to create industrial materials. The crystalline limestone is one of the sedimentary rocks in the limestone hills. This research is conducted to investigate the impact of dolomitization around Kinta Valley in terms of sedimentology and petrography especially in northern part of Sungai Siput, Perak. The research was divided in two phases; first phase focused on general geology. The second phase focused on laboratory analysis and other studies to get insight of the dolomitization process. The results showed facies types, presence of dolomitization, FTIR graph, SEM photo and EDS results.

ACKNOWLEDGEMENT

First of all, I would like to express my gratitude to my Final Year Project Advisor, AP. Dr. Eswaran Padmanabhan for his assistance in completing this project throughout the entire length of this project. Highest gratitude is also for the late Dr. Essam Mansour, at which to whom this project is dedicated as the title were one of his final ideas before his early passing. May he rest in peace.

I also would like to thank my parents, all lecturers and dear friends who have been very supportive in these 5 years of my study in Universiti Teknologi PETRONAS. The experience gathered during this time is priceless and is hoped to help in helping me to become a professional in the oil and gas industry.

The final year project is a great exposure especially to us, Petroleum Geoscience students, at which the project helps us to implement and to test theories learnt in classroom into practice, thus securing the knowledge to ourselves. In the project titled “General Geology of the Carbonate within a quarry in northern part of Sungai Siput, Perak with an emphasis on Dolomitization”, I have learnt a lot in conducting a geological fieldwork as well as conducting a number of tests to confirm the ideas and hypotheses based on the observation of the study area. And it is hoped that the project can be used and useful to the geological community today.

Here, I also would like to acknowledge all the personnel who at which have helped me in completing this project directly or indirectly. Special thanks to AP Askury Abdul Kadir, Mr. Solomon and not to forget the staff of Jabatan Mineral dan Geosains, Ipoh, Perak Darul Ridzuan for their guidance given.

Finally, I would like to express my gratitude to Universiti Teknologi PETRONAS for designing a course structure as useful as this. The experience is really beneficial in preparing ourselves before becoming industry players.

TABLE OF CONTENTS

CERTIFICATION	i
ABSTRACT	ii
ACKNOWLEDGEMENT	iii
CHAPTER 1: INTRODUCTION	1
1.1 Background of Study	1
1.2 Problem Statement	3
1.3 Objectives and Scope of Study	3
CHAPTER 2: LITERATURE REVIEW/THEORY	4
2.0 General geology of Kinta Valley	4
2.1 Limestone	4
2.2 Granite	5
2.3 Diagenetic process and Dolomitization	5
CHAPTER 3: METHODOLOGY	7
3.1 Field Map	7
3.2 Topographic Map	8
3.3 Stereonet	8
3.4 Cross-section	8
3.5 Facies Logging	8
3.6 Total Carbon	8
3.7 Thin-section petrography study	9
3.8 X-ray diffraction (XRD)	9
3.9 Scanning electron microscopy (SEM)	9
3.10 Energy-dispersive X-ray spectroscopy (EDS)	9
3.11 Fourier Transform Infrared Spectroscopy (FTIR)	9
CHAPTER 4: RESULTS AND DISCUSSION	11
4.1 Results and Discussion	11
CHAPTER 5: CONCLUSION AND RECOMMENDATION	35
5.1 Conclusion	35
5.2 Recommendations	35

REFERENCES	37
APPENDICES	39

LIST OF FIGURES

Figure 1	Geological map of the limestone hills	11
Figure 2	Cross section of Line 1	12
Figure 3	Stereonet with lines and planes	13
Figure 4	Rose diagram of the strike/dip in the quarry	13
Figure 5	Sedimentary log of the limestone hill in quarry	17
Figure 6	Thin section of sample 3 (Magnification: 4x)	19
Figure 7	Infrared spectrum of reference chemical compounds	24
Figure 8	Infrared spectra of the calcite and dolomite groups	25
Figure 9	Infrared spectra of the calcite and dolomite groups	25
Figure 10	Infrared spectra of facies L4 and RU2 in quarry	27
Figure 11	XRD result of facies L4	29
Figure 12	The SEM photo and EDS spots and map of facies RU1	31
Figure 13	EDS graph of facies Ru1 at spot 1 (red star)	32
Figure 14	EDS graph of facies RU1 at yellow spot 2	32
Figure 15	EDS graph of facies RU1 in yellow square map	33
Figure 16	The geological map of Kinta Valley	39
Figure 17	FTIR graph of facies N4	40
Figure 18	FTIR graph of facies RU4	41
Figure 19	FTIR graph of facies RU1	42
Figure 20	FTIR graph of facies RU3	43
Figure 21	Thin section of sample 1(Magnification: 4x)	44
Figure 22	Thin section of sample 2 (Magnification: 10x)	45
Figure 23	Thin section of sample 3 (Magnification: 4x)	46
Figure 24	Thin section of sample 4 (Magnification: 4x)	47
Figure 25	Thin section of sample 9 (Magnification: 4x)	48
Figure 26	Thin section of sample 11 (Magnification: 4x)	49

Figure 27	Analysis Report of Total Carbon of L4	50
Figure 28	Analysis Report of Total Carbon of N4	51
Figure 29	Analysis Report of Total Carbon of RU1	52
Figure 30	Analysis Report of Total Carbon of RU4	53
Figure 31	Analysis Report of Total Carbon of RU2	54
Figure 32	Analysis Report of Total Carbon of RU3	55
Figure 33	XRD result of N4	56
Figure 34	XRD result of RU1	57
Figure 35	XRD result of RU2	58
Figure 36	SEM and EDS photo with spot and map EDS analysis of RU2	59
Figure 37	EDS graph of facies RU2 at spot	60
Figure 38	EDS graph of facies RU2 at map	61
Figure 39	SEM and EDS photo with spot and map EDS analysis of RU3	62
Figure 40	EDS graph of facies RU3 at white spot	63
Figure 41	EDS graph of facies RU3 at square map	64
Figure 42	SEM and EDS photo with spot and map EDS analysis of RU4	65
Figure 43	EDS graph of facies RU4 at white spot	66
Figure 44	EDS graph of facies RU4 at red spot	67
Figure 45	EDS graph of facies RU4 at square map	68
Figure 46	The picture of outcrops at quarry in Sungai Siput	69
Figure 47	Photo of the hills and facies labels	70

LIST OF TABLES

Table 1	Summary of the descriptions of the thin sections	18
Table 2	Summary of total carbon	20
Table 3	Reference chemical compound	21
Table 4	Calcite and dolomite groups	21
Table 5	Positions of Absorptions Bands of six samples	25
Table 6	Table of EDS analysis of facies RU1	28
Table 7	Table of EDS analysis of facies RU1	29
Table 8	Table of EDS of facies RU1 in yellow square map	29
Table 9	Table of EDS analysis of facies RU2 at the spot	60
Table 10	Table of EDS analysis of facies RU2 at map	60
Table 11	Table of EDS analysis of facies RU3 at white spot	62
Table 12	Table of EDS analysis of facies RU3 at square map	62
Table 13	Table of EDS analysis of facies RU4 at white spot	64
Table 14	Table of EDS analysis of facies RU4 at red spot	64
Table 15	Table of EDS analysis of facies RU4 at square map	65

CHAPTER 1

INTRODUCTION

1.0 INTRODUCTION

This research is about investigation of dolomitization impact in quarry of Sungai Siput, Perak based on several geological laboratory methods and at the same time to create a map of lithology of the area. Generally, diagenesis may comprise all processes that convert sediment to sedimentary rock. It is a continual active process involving sediments where the composition of sedimentary mineral react to gain an equilibrium with surrounding pressure, temperature and chemistry, slowly changing its properties. Prior to the diagenesis, porosity and permeability are controlled during deposition by composition and surrounding conditions. Dolomitization is one of the diagenetic processes that may be occurs in the study area.

1.1 BACKGROUND

Area of Sungai Siput is surrounded several limestone hills where several quarries has been operated years back. The quarry that we interested is around Sungai Siput. In this quarry, the operator is quarried magnesium oxide which the limestone overthere is rich-in magnesium oxide and the dolomite mineral may take place in the mineral composition; dolomitization may occur. The common features of the limestone overthere are light grayish white limestone.

Limestone is a sedimentary rock composed mainly of calcium carbonate, CaCO_3 and this mineral made up the majority of formation found in Kinta Valley, Perak (Tan, 2010). All the limestone mountainous hills are what remain from the limestone beds that were eroded which formed around Paleozoic (Ordovician to Permian). The karst features are presented due to the karstification or dissolution of limestone by meteoric water. The Kinta Valley limestone is estimated about 3000 meters thick and interbedded to each other with dolomite, black shale, and carbonaceous shale and also carboniferous limestone as its succession. Structurally, the formation is highly folded and faulted and there are regions of which the limestone has been metamorphosed due to direct contact with igneous body found in the western belt of the Main Range.

The diagenesis of carbonate sediments encompasses all the processes that affect the sediments after deposition up to the realms of metamorphism at elevated temperatures and pressures (Moore, 2001). When carbonate sediments undergo shallow to intermediate burial diagenesis, meteoric diagenetic pathways are important for major diagenetic changes (Land, 1986). These days, however, the quest for reservoir quality calls for a deliberate focus on diagenesis where it will ultimately determine the commercial viability of a reservoir in terms of combined effect of burial, bioturbation, compaction and chemical reactions between rock, fluid and organic matter. Furthermore, exploration and production have used core analysis and petrophysical examination and gain many benefits from these studies to overcome the effects of diagenetic cements. Diagenesis has been to subject of research and discussion since several years ago to glean more information and gain greater understanding of the reservoirs. Moreover, the dolomitization; one of the diagenetic processes is a process where calcite be replaced by dolomite; dolomite is formed when magnesium ions replace calcium ions. In the sabkha area, it is common for mineral alteration due to the evaporation of water. Dolomitization involves substantial amount of recrystallization.

1.2 PROBLEM STATEMENT

The northern area of Sungai Siput, Perak is lack of study in terms of geological studies, whereas many studies only focused in other parts of Kinta Valley. This study only focused at the northern part of Sungai Siput where currently a quarry company is operating to extract magnesium oxide from the limestone hills. The area is consists several cluster of limestone hills, however only the middle hills is been quarrying due to high-rich of magnesium. This study is conducted to answer what the effect of dolomitization impact upon the reservoir properties of carbonate rock and what are the mineral composition and chemical composition present in the study area.

1.3 OBJECTIVES AND SCOPE OF STUDY

- To study the general geology and dolomitization on the carbonate rock at the northern part of Sungai Siput, Perak and is to identify the chemical and mineral compositions of the limestone in the area.

CHAPTER 2

LITERATURE REVIEW/THEORY

2.0 GENERAL GEOLOGY OF KINTA VALLEY

In general, the floor of Kinta is made up of Old Alluvium (Simpang Formation) overlain by Younger Alluvium (Beruas Formation) (Raj et al 2009). In this thick alluvium, the rich sedimentary tin ores were concentrated and mined. The exposed bedrock of the valley is made up of older metamorphic rocks or sometimes stood up as isolated hills, while intrusive rocks form mountains on both eastern and western slopes of the basin. Ingham and Bradford (1960) described and illustrated the geology of Kinta Valley.

Based on Abd. Kadir et al. (2008), during Silurian, clastic sediments deposited in a relatively deep marine setting, this area were followed by a limestone deposition in a progressively shallowing marine condition. The evidence of the depositional environment hypothesis is supported by the presence of rich shallow marine benthic organisms within the Kinta Limestone from Devonian to Permian age. During Late Triassic to early Jurassic, acidic igneous rock intruded the older rock formations. Thus, it formed the Main Range, Kledang Range and Bujang Melaka Granites. Furthermore, the intrusion was responsible in the transformation of the older sedimentary rocks into marble and schist. Following the collision of Sibumasu – East Malaya, Peninsular Malaysia was uplifted to form terrestrial environment. Thus,

allowed exogenic processes to take place and karst formation formed around the Kinta Valley.

2.1 Limestone

Limestone is a sedimentary rock composed mainly of calcium carbonate, CaCO_3 and this mineral made up the majority of formation found in Kinta Valley, Perak (Tan, 2010). All the limestone mountainous hills are what remain from the limestone beds that were eroded which formed around Paleozoic (Ordovician to Permian). The karst features are presented due to the karstification or dissolution of limestone by meteoric water. The Kinta Valley limestone is estimated about 3000 meters thick and interbedded to each other with dolomite, black shale, and carbonaceous shale and also carboniferous limestone as its succession. Structurally, the formation is highly folded and faulted and there are regions of which the limestone has been metamorphosed due to direct contact with igneous body found in the western belt of the Main Range.

2.2 Granite

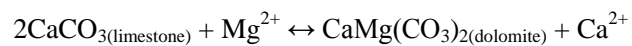
Granite is an igneous rock (Wikipedia, 2014). The granite commonly has granular and phaneritic in texture. The compositions of granite are quartz, mica and feldspar. Some individual crystals are larger than groundmass, may know as porphyritic or poryphyrr. The colors of granite usually pink to gray which depending on their rheology, chemistry and mineralogy. However, granite is differs from granodiorite; at least 35% of the feldspar in granite is considers as alkali feldspar. The alkali feldspar gives granite distinctive color of pink. Granite in the Kinta Valley is located at the Main Range. The granite body was direct contact with the surrounding rock formations; in this case, it is limestone. Thus, it is explained why the limestone has crystalline-like look and some of them is metamorphosed into marble.

2.3 Diagenetic process and Dolomitization

The diagenesis of carbonate sediments encompasses all the processes that affect the sediments after deposition up to the realms of metamorphism at elevated temperatures and pressures (Moore, 2001). When carbonate sediments undergo shallow to intermediate burial diagenesis, meteoric diagenetic pathways are important for major

diagenetic changes (Land, 1986). These days, however, the quest for reservoir quality calls for a deliberate focus on diagenesis where it will ultimately determine the commercial viability of a reservoir in terms of combined effect of burial, bioturbation, compaction and chemical reactions between rock, fluid and organic matter. Furthermore, exploration and production have used core analysis and petrophysical examination and gain many benefits from these studies to overcome the effects of diagenetic cements. Diagenesis has been a subject of research and discussion since several years ago to glean more information and gain greater understanding of the reservoirs.

The dolomitization is a process where calcite is replaced by dolomite; dolomite is formed when magnesium ions replace calcium ions. In the sabkha area, it is common for mineral alteration due to the evaporation of water. Dolomitization involves a substantial amount of recrystallization:



This process depends on specific conditions which include low Ca:Mg ratio in solution, reactant surface area, high temperature, the mineralogy of the reactant and the presence of kinetic inhibitors.

CHAPTER 3

METHODOLOGY/PROJECT WORK

For the first part of final year project I (FYP I), a lithology map basis on available topography map, in the lithology boundary map, geoscientist enable to determine the rock types presented in the Kinta Valley as well as the extension of the rock formation. As for the information gathering, a field work will be conducted where the strike and dip of the formations will be collected. The data gathered is then being used to develop the geological map of the area.

For the geological fieldwork in FYP 1, among the required equipment are; geological hammer, compass, magnifying lens and Global Positioning System device (GPS).

3.0 General Geology

3.1 Field Map

The map is shown geologic features of certain area. Rock units or geologic strata may show in the map depend the available data and symbolised using colours or symbols where they are exposed. Other geologic features such as bedding planes and structural features (e.g.: folds, foliation, lineation and faults) shown by strike and dip. It is the symbology of lithologies and orientations.

3.2 Topographic Map

The topographic map is a large-scale detail and quantitative characterized map of representation of relief using contour lines. A contour line represents elevation on a topographic map, directly we know the height of the terrains.

3.3 Stereonet

The stereonet used in the study is focused in structural analysis using strike/dip data, poles concentration to identify the structural existed in the study area. It is a stereographic projection using equal-area stereonets. The stereonet is used to find the intersection between two planes, the angle between two lines and restored orientation of geologic features and bisect the angle between two planes.

3.4 Cross-section

The function of the cross section is to view the Earth as if it were cut open and seen from the side. The cross sections are interpretative as the observation cannot be observed directly. The terrains such as canyons or high mountains or even hilly areas can natural cross sections.

3.5 Facies Logging

Using the stratigraphic/sedimentological/core description log sheet where the facies logging is done by observation in the fields. The observed lithology will be recorded in the log sheet and show any litho-facies changes in the fields.

Secondly, a number of tests was conducted. The details of deformation such as cementation, dissolution and diagenesis of the gathered samples are usually, for the most part been revealed in the laboratory, where various analyses were conducted during FYP II period.

3.6 Total Carbon

Total carbon (TC) is the amount of carbon bound on in other word it is the quantity of organic matter in an organic compound in a source rock and been determined by a

LECO Carbon Analyser and measured in wt%. Furthermore, TC also called organic carbon (C org). It measures the quantity but not the quality of organic carbon in rock or sediment samples. This is a misconception about the minimum TC required for carbonate source rocks is less than that for shale source rock. However, that is no significant differences in minimum TC exist between non-carbonate and carbonate sediments.

3.7 Thin-section petrography study

It is a basic technique usually been used to examine the textural characteristics of rock. Firstly, rock samples are cut to thin slices, which are polished and impregnated with epoxy resin to enhance porosity identifications. The thin-section slides are studied under filtered polarizing light using a polarized light microscope.

3.8 X-ray diffraction (XRD)

The principle of this technology works on unique diffraction pattern produced by each crystalline substance. When a rock is ground into powder form, each component will produce a unique pattern independently to each other, or in a simple word, it provides a fingerprint of each component which enables to identify the mineralogical makeup of the sample. Thus, the XRD is capable to reveal the crystallographic structure and chemical composition of the rock or clay fraction.

3.9 Scanning electron microscopy (SEM)

The analysis by Scanning Electron Microscopy focused in a wide range of magnification for identifying minerals. Addition to that, SEM provides geoscientist to investigate pore morphology and pore throat geometry. The SEM technique enable us to photograph the distribution of detrital and authigenic mineral and provide the effect study of cementation and coatings on porosity.

3.10 Energy-dispersive X-ray spectroscopy (EDS)

EDS is an analytical technique used in elemental analysis or chemical characterization of a sample. This technique relies on interaction between X-ray

excitation and a sample. The fundamental of the principle based on a unique atomic structure which allowing unique set of peaks of X-ray spectrum.

3.11 Fourier Transform Infrared Spectroscopy (FTIR)

FTIR is a technique used to obtain infrared spectrum of absorption, emission, photoconductivity or Raman scattering of a substance (in form of solid, liquid or gas). An FTIR spectrometer collects spectral data in a wide spectral range. The objective of FTIR is to measure how well a sample absorbs light at each wavelength.

CHAPTER 4

RESULTS AND DISCUSSION

4.1 Geological Map

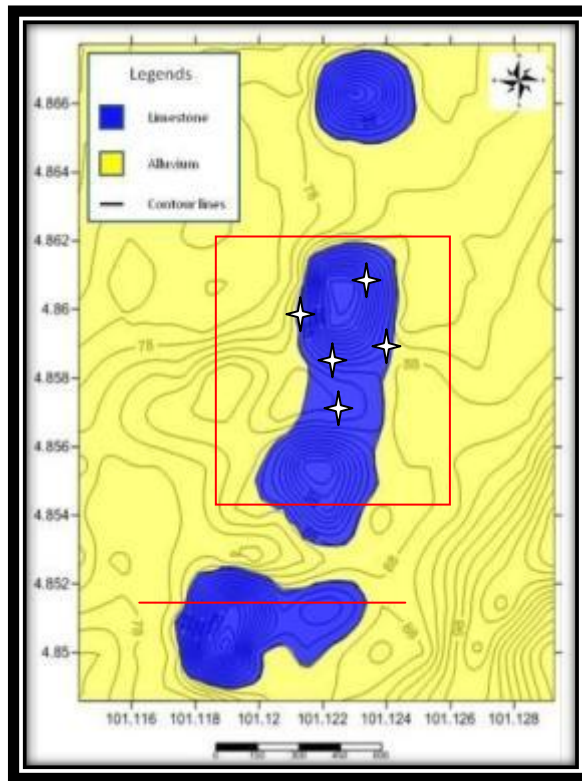


Figure 48: Geological Map of the limestone hills at northern part of Sungai Siput, Perak

Figure 1 shows the limestone hills at northern of Sungai Siput Perak. The “star” symbols represent the outcrops presented and the red square indicated the area studied. Several samples have been examined and collected for further analyses. The blue and yellow represent limestone and alluvium respectively. The size of the map is 2x3 km with a scale of 1 cm to 150 m. At the eastern direction of the limestone hills, located Main Range of Malaysia; Banjaran Titiwangsa. The latitude of the map in range of 4°85’N to 4°866’N, meanwhile the longitude of the map in range of 101°116’ to 101°128’. The map is generated using the GPS reading basis on the coordinates and elevation during fieldtrip and road traversing at the area. The contour map is generated by Surfer software where the coordinate and elevation values taken are inserted. The lithologies of the map area are limestone and alluvium and the surrounding environment is covered with palm oil tress plantation.

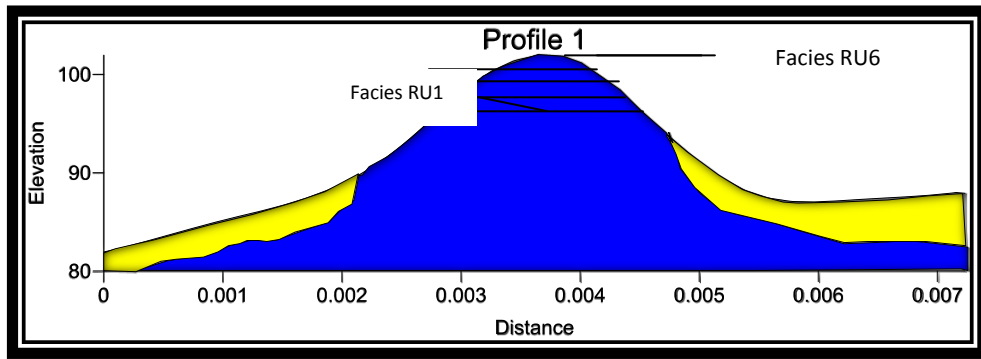


Figure 49: Cross section of Line 1 (Red Line in Figures 1)

Figure 2 shown a cross section based on line 1 (red line) in Figure 1. The blue area is indicated as limestone and yellow is alluvium surrounding the limestone hills. The extension of the limestone rock unit is assumed based on previous model by Jabatan Geosains and Mineral Malaysia and also the interviews with the quarry works overthere. For line 1 (red line), there is no structural reading such as strike and dip due to no access to the exposed outcrop and quarry hazard around the hill.

4.2 Stereonet

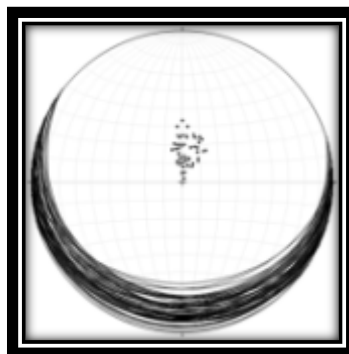


Figure 50: Stereonet with lines and planes

The planes plotted on the stereonet are shown all the planes concentrated at the south-west direction. The system that can identify is an open fracture which concentrated at south-west direction.

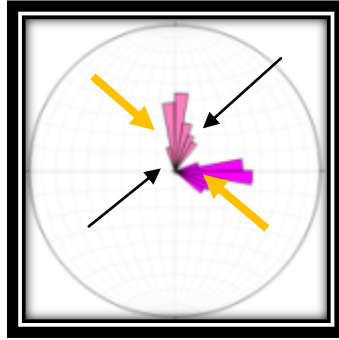
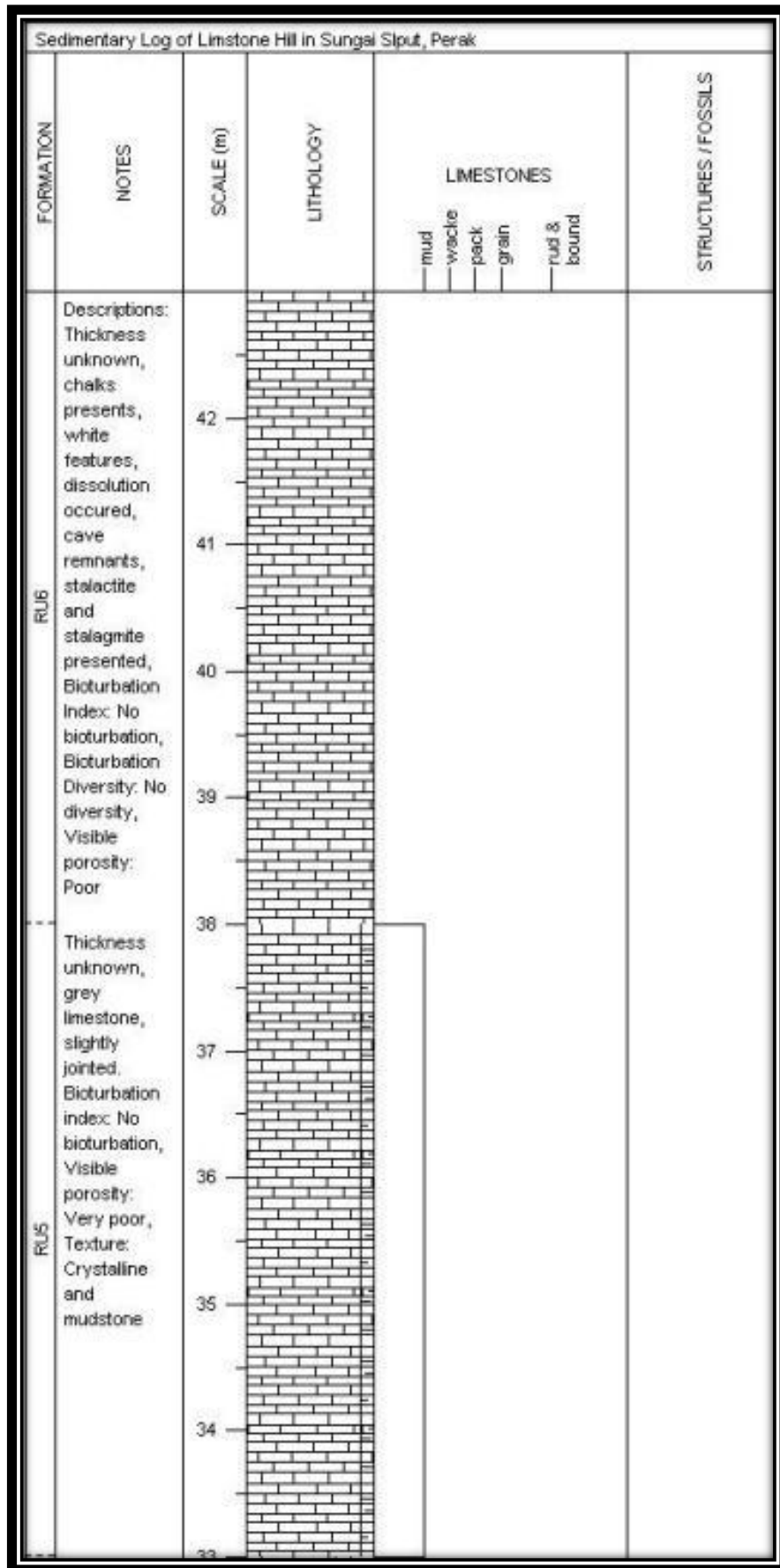
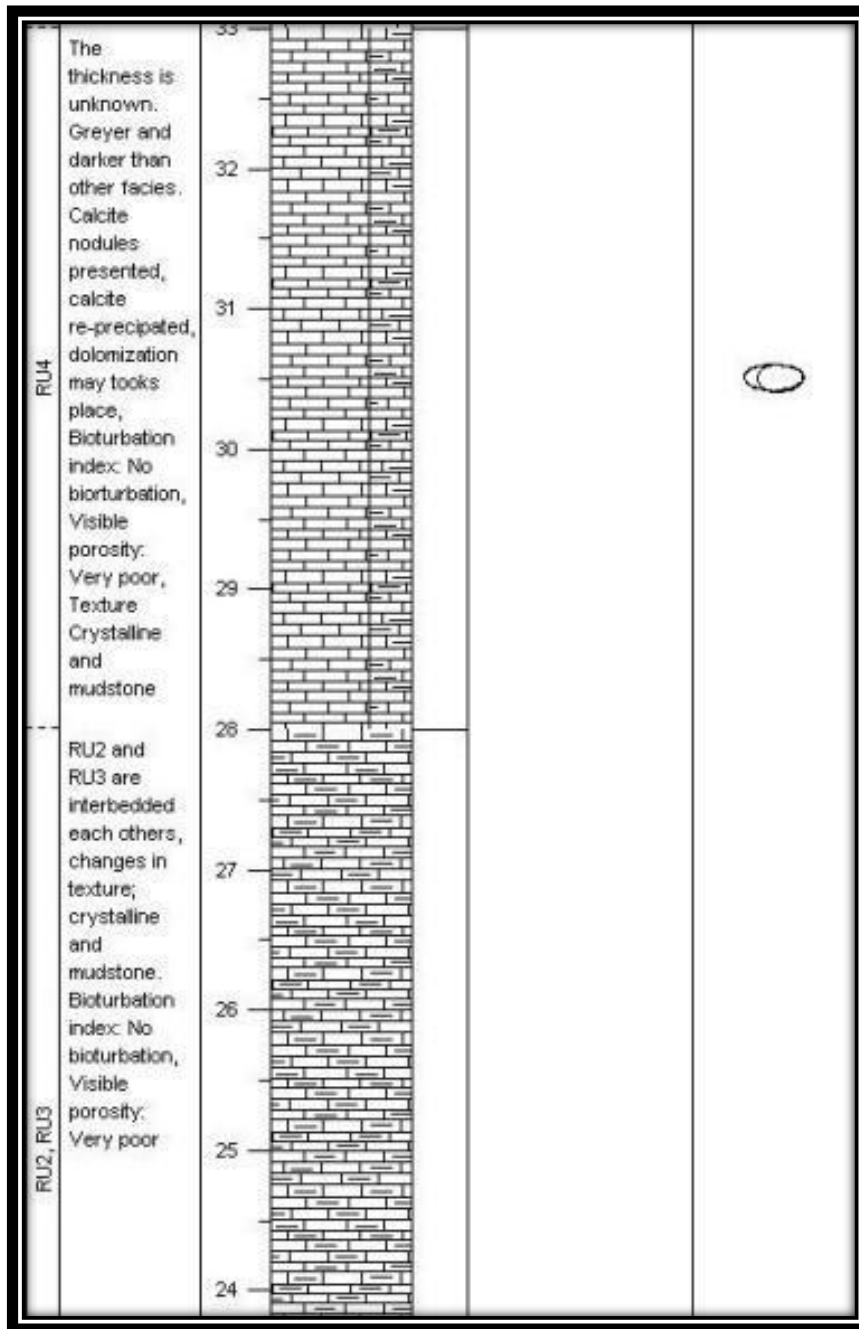


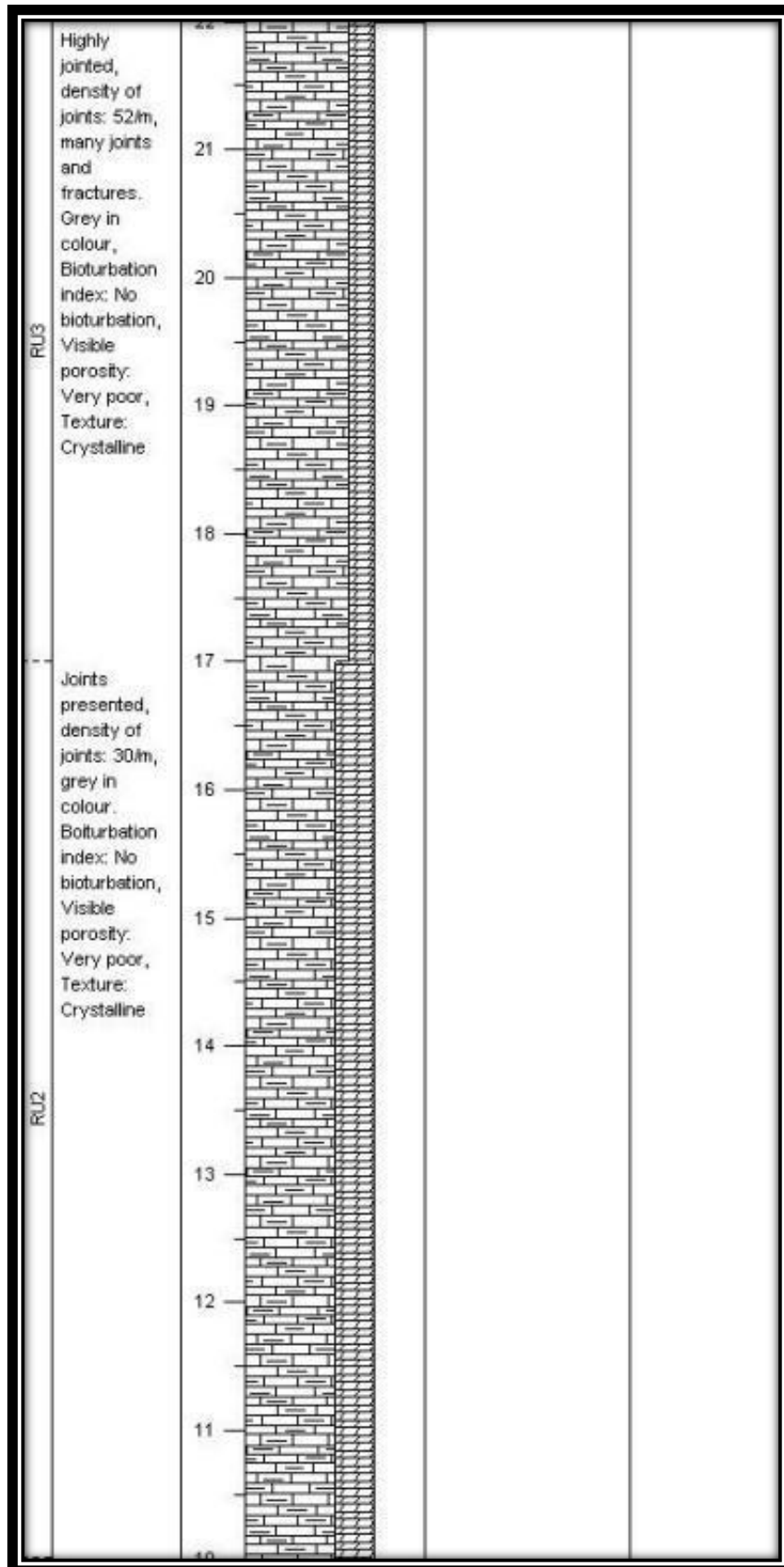
Figure 51: Rose diagram of the strike/dip in the quarry

Based on Figure 2, Sigma 1 is represented by black arrows meanwhile for Sigma 3 is symbolised by orange arrows. The Sigma 1 indicated the extension or compression direction of stress/strain. Sigma 1 is directed from north-east and south west direction, meanwhile, Sigma 3 is from the north-west and south-east direction.

4.3 Facies logging







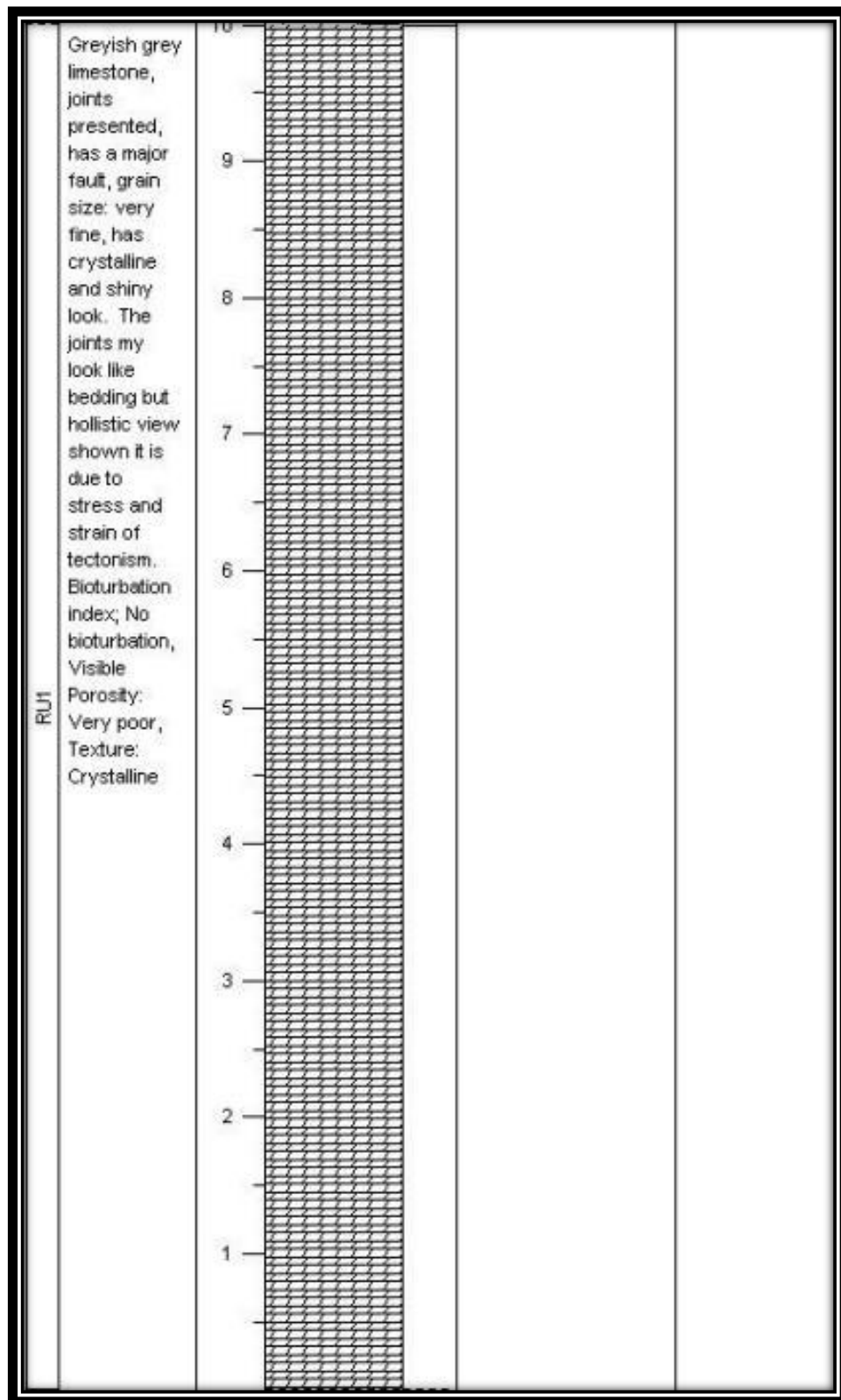


Figure 52: The sedimentary log of the limestone hill in quarry, Sungai Siput, Perak

The complete succession of the limestone hill in Sungai Siput, Perak is summarised in the above figure. In general, the limestone hill have been recognized into seven facies on the basis of its rock type, sedimentary textures and structures, bedding

contacts, bedding thickness as well as fossil contents. These facies are RU1, RU2, RU3, RU2/RU3, RU4, RU5 and RU6. These lithofacies are plotted in the sedimentary log to interpret the sedimentary or diagenetic processes. In general, the lower part of the succession comprises of greyish grey limestone with has crystalline and shiny surface, joints presented on the facies. This part of lower succession is dominated by facies RU1, RU2 and RU3. Moreover, facies RU2 and RU3 showed highly joints features on the facies surfaces with 30/m and 52/m respectively. Towards the middle part of the succession, the facies gradually mixed between RU2 and RU3 where these two facies are interbedded to each other and have a very similar texture, colour with lower succession of RU1, RU2 and RU3. In the upper part of the succession, the facies are characterized by thick limestone facies of RU4, RU5 and RU6. RU4 and RU5 facies have similar textures; crystalline texture. However, in facies RU4, calcite nodules are presented and thus differentiate it from facies RU5. Facies RU6 is the topmost succession of the upper part of the succession and has unique features. The common features at facies RU6 is karst features; stalagmites and stalactites. These features indicated the cave remnants at the top of the hill and the dissolution of the limestone due to weathering process where the topmost succession is most exposed facies than others. Furthermore, six facies shared similar features which are greyish grey in colour, crystalline-like textures and the grain sizes are quite same. Addition, bioturbation index is zero (no bioturbation) and very poor of visible-porosity in all facies. The field pictures labels of the facies are attached in Appendices.

4.4 Thin section

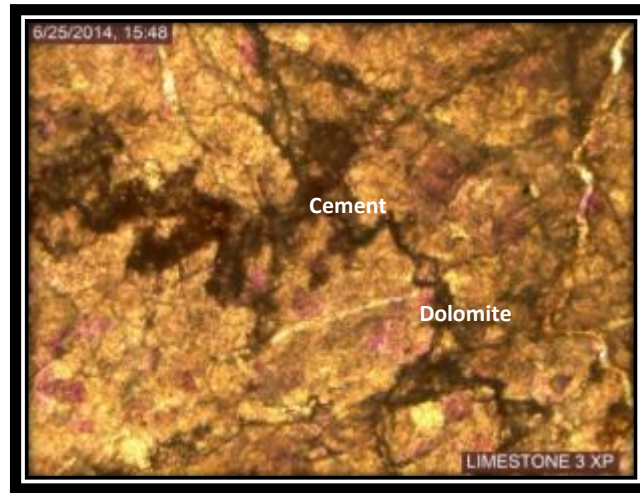


Figure 53: Thin section of sample 3 (Magnification: 4x)

Table 16 Summary of the descriptions of the thin sections

Samples	Texture	Components	Outcrop Structure	Interpretation/Remarks
Sample 1	Crystalline, matrix?	Unidentified	Exposed surface, cave remnant?	Dolomitization?
Sample 2	Crystalline, matrix?	Unidentified	Exposed surface, parallel bedding	Dolomitization?
Sample 3	Crystalline, matrix	Unidentified	Exposed beds	Dolomitization?
Sample 4	Crystalline, matrix?	Unidentified	Exposed beds	Dolomitization?

Sample 9	Crystalline, mud matrix?	Unidentified	Exposed beds	Dolomitization?
Sample 11	Crystalline, grain-supported, calcite veins?	Calcite, crystallised grain?	Cave remnants	Dolomitization?, calcite intrusion

The table below shows summary of all six samples and the above figures shows the photo of sample 3 under magnification of 4x. Other photos of the samples are attached in the Appendix. The crystalline structure under the microscope show calcite was replaced by crystalline-like structure probably dolomite via dolomitization and several intrusions such as calcite or quartz veins. Sample 1 to sample 11 is in basis of order from the lower succession to upper succession of the limestone hills respectively. Thus, the outcrop for each sample is different. Limestone contains carbonate minerals which including CO₃ anion and combines with cations such as Ca, Mg, Fe, Mn and Zn to form most carbonate minerals. The common carbonate minerals can be found are calcite group, dolomite group and aragonite group. These three minerals are the only volumetrically important minerals in carbonate rocks. Under thin section analysis, calcite, dolomite and aragonite are expected to be seeing under microscope. Thus, to distinguish between calcite, aragonite and dolomite in hand specimens and thin sections is difficult due to their physical characteristics are very similar.

In this study, calcite and dolomite is highly expected to cross in all collected samples than aragonite due to the quarry operator mentioned earlier they extracting magnesium oxide at the limestone hill area. Under the microscope, several properties between calcite and dolomite to visually differentiated them.

The properties of calcite are hexagonal-like crystal system, have perfect rhombohedral cleavage, its colour usually white/colourless in hand samples and colourless in plane polarized light, have moderate to high negative relief, high-order interference colours which is commonly white. Meanwhile, the properties of

dolomite are hexagonal-like crystal system, have perfect rhombohedral cleavage, its colours may in pink, white, gray, green, brown, black or colourless, its crystals are usually subhedral to euhedral with planar boundaries. All the calcite and dolomite properties are highly considered during thin section analysis.

Thus, the dominant properties that can be seen under the polarized microscope are colourless in thin section but sometimes there is pink in colour presented. The crystal system is more subhedral to euhedral. Hence, the assumed mineral presented and can be seen under the microscope is more resembled to dolomite properties. For further confirmation, others analysis is used such as SEM, EDS, FTIR and XRD.

4.5 Total Carbon

The table below showed the total carbon in six (6) samples. The peak graph of total carbon is shown in Appendices.

Table 17 Summary of total carbon

Samples	Total Carbon (%)	Total Carbon I [AU]
L4N9	11.5	1.014E6
No. 4	12.1	1.078E6
R1 No.1	11.4	1.069E6
R4 No.11	11.9	1.049E6
RU2	12.3	1.082E6
RU3	11.1	9.828E5

The above table shows the total carbon contain in each sample and provide quantitative analysis for the carbon that may contain in the samples. The total carbon values of the samples are ranging from 11.1% to 12.3% from total contents in the samples. Thus, it prove the carbon element is presented in the limestone samples.

4.6 Fourier Transform Infrared Spectroscopy (FTIR)

Table 18 Reference chemical compound (Huang et al., 1960)

No.	Chemical Compound	Positions of Absorptions Bands (cm-1)
1	KBr	3510; 2990; 2410-2300; 1667-1456; 1110;
2	MgO	1493; 1429; 885; 800
3	CaO	3510; 1493-1429
4	Na ₂ CO ₃	2530; 1795; 1450; 881; 702-694

Table 19 Calcite and dolomite groups. (Huang et al., 1960)

No.	Mineral	Positions of Absorptions Bands (cm-1)
1	Magnesite	1818; 1450; 887; 748
2	Smithsonite	2530; 1830; 1440; 870;743
3	Siderite	1818; 1422; 866; 737
4	Rhodochrosite	2530; 1810; 1433; 867; 727
5	Calcite	2545; 1812; 1435; 879; 712
6	Calcite	2550; 1818; 1435; 878; 713
7	Dolomite	2530; 1818; 1450; 881; 730
8	Ankerite	2530; 1825; 1450; 877; 726

9	Kutnahorite	2520; 1818; 1435; 869; 721
---	-------------	----------------------------

Each carbonate shows unique characteristics of absorption bands which some are differ more or less from published or studied curves. Huang et al. (1960), the spectral difference between the common minerals may be due to crystal structure. The above tables (Table 3 and Table 4) are the summary studies of the infrared spectra of carbonates minerals and chemical compounds by Huang et al. (1960) to furnish systematic data on the infrared spectra of these carbonate minerals and also to infer in general terms the correlation between spectral changes and internal structure. Below figure shows infrared spectrum of reference chemical compounds by Huang et al. (1960).

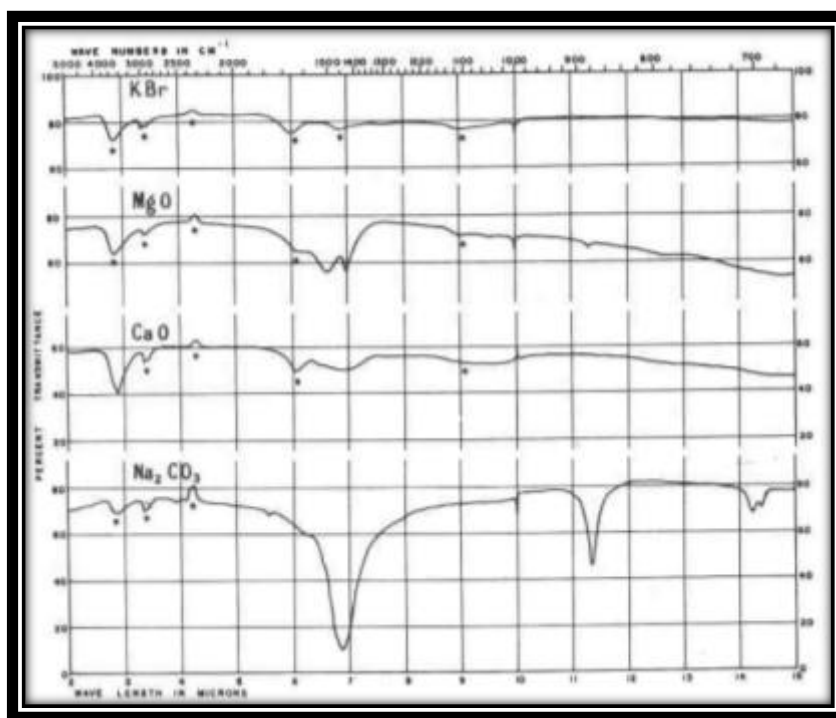


Figure 54: Infrared spectrum of reference chemical compounds (Huang et al., 1960)

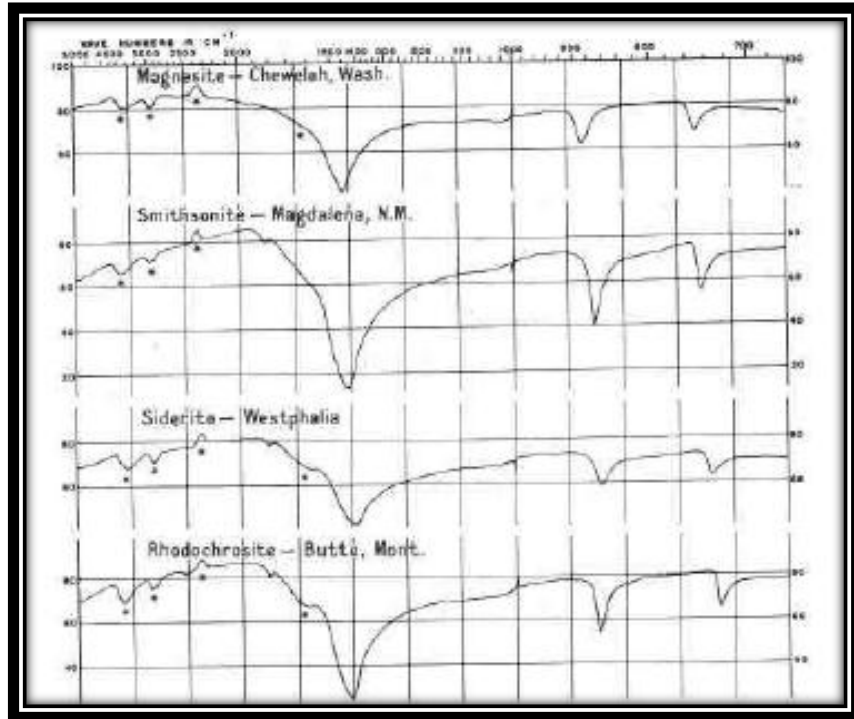


Figure 55: Infrared spectra of the calcite and dolomite groups (Huang et. al., 1960)

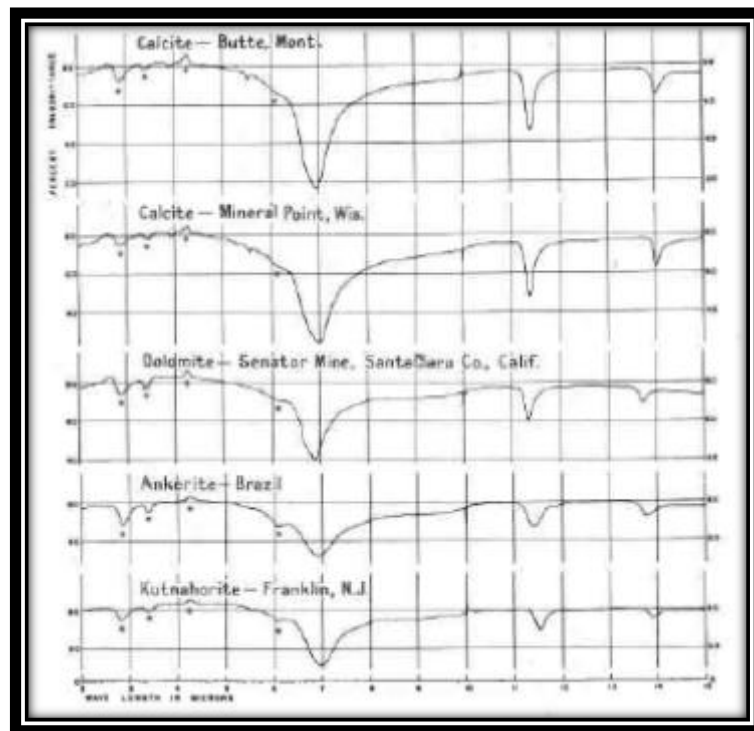


Figure 56: Infrared spectra of the calcite and dolomite groups (Huang et. al., 1960)

Based on the Huang et al. (1960) studies, the above three figures (Figures 7, 8 and 9) are the basis of the FTIR analyses of six samples to determine the mineral and chemical compositions of the collected limestone rock.

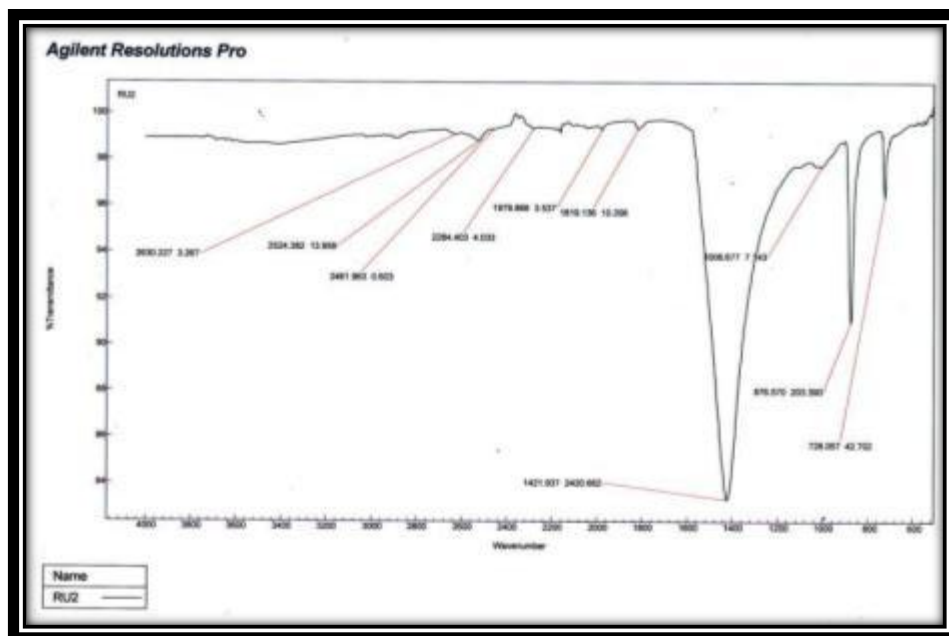


Figure 57 FTIR results of RU2

Figure 10 shows one of the six graphs of FTIR that has been conducted for six samples and the other graphs are attached in the Appendix. For every peaks of the FTIR graphs, the value of the positions of absorptions bands (cm-1) is recorded in the below table. The recorded values of the six graphs are later on compared with the study of Huang et al. (1960).

Table 20 Positions of Absorptions Bands of six samples of the limestone hills

No.	Samples	Positions of Absorptions Bands (cm-1)
1	L4	2888.547; 2627.841; 2526.095; 2283.258; 1818.809; 1422.024; 1099.950; 876.747; 876.747; 727.972
2	No. 4	2526.538; 2453.994; 2282.614; 1421.067; 876.840; 727.987
3	R1	2888.994; 2626.573; 2526.375; 2454.563; 2283.501;

		1820.021; 1424.960; 995.050; 877.508; 728.121
4	RU2	2630.227; 2524.382; 2461.963; 2284.403; 1979.868; 1819.136; 1421.937; 1008.677; 876.570; 728.057
5	RU3	2628.431; 2525.918; 2359.069; 2162.693; 1819.626; 1420.519; 876.574; 728.051;
6	RU4	2627.547; 2522.826; 2455.484; 2282.866; 1979.511; 1415.299; 975.271; 728.110

Thus, from the FTIR result of the six (6) quarry samples; the value of the positions of absorptions bands (cm-1) which shown resemble as in dolomite mineral's positions of absorptions bands. Therefore, in all six samples most probably composes of high-rich dolomite mineral.

4.7 X-ray Diffraction (XRD)

The four samples from FTIR which included L4, N4, RU1 and RU2 is tested using XRD analysis to determine the chemical composition of the samples. The XRD results that generated is later on been compared with standard patterns database using EVA software. The result for L4 as below:

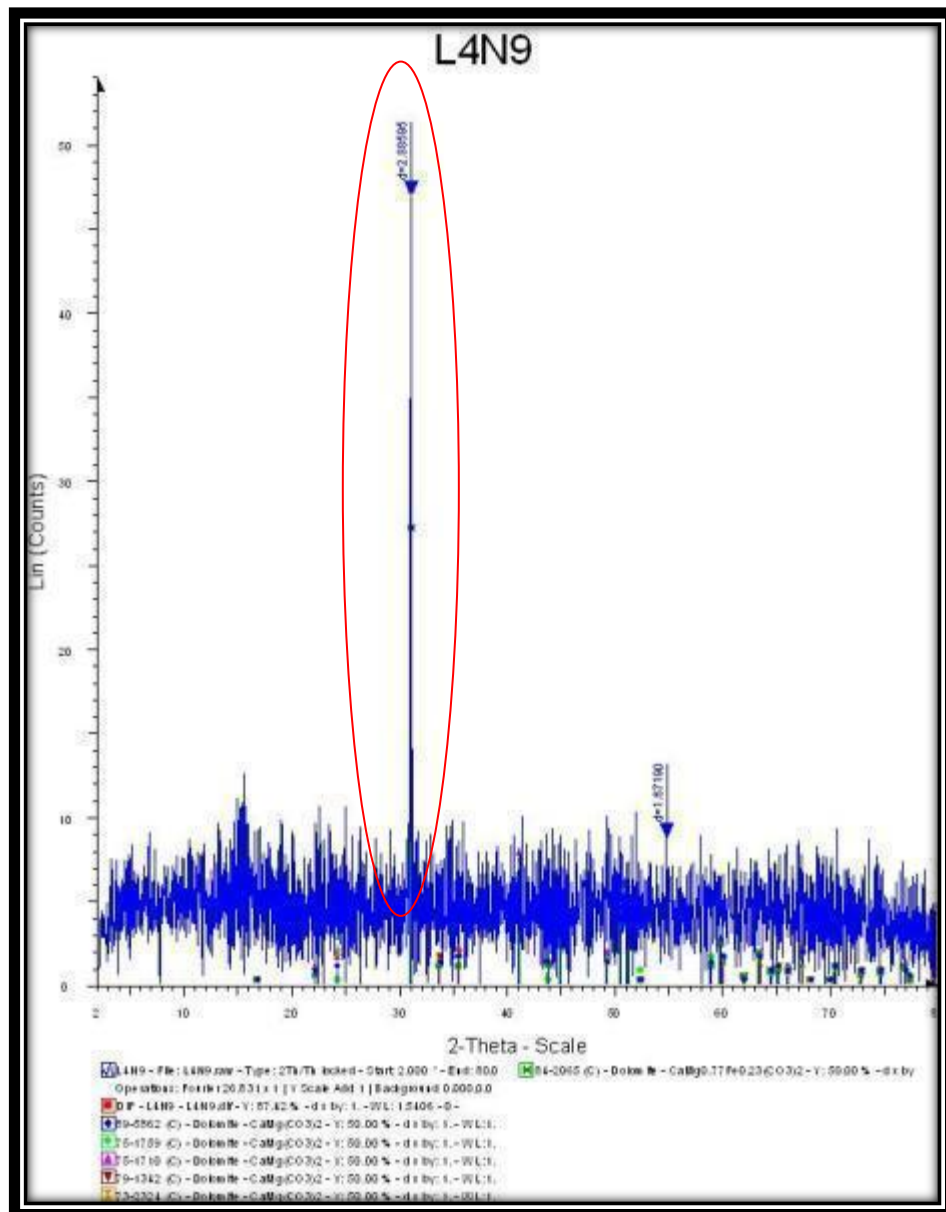


Figure 58: XRD result of facies L4

The peak of XRD results for four samples (L4, N4, RU1 and RU2) is peaked at almost same value of 2-Theta-Scale, which are around 30-32. After done with EVA software for evaluate and interpreted the XRD results, the “Search Match” functions

shown pattern results of dolomite ($\text{CaMg}(\text{CO}_3)_2$) in four samples. Below the L4 result, there are legends shown dolomite similar-like pattern with the L4 result. Thus, the predominantly composition in four samples is dolomite. The others three figures shown N4, RU1 and RU2 are attached in Appendix.

4.9 Scanning electron microscopy (SEM) and Energy-dispersive X-ray spectroscopy (EDS)

RU1 SEM

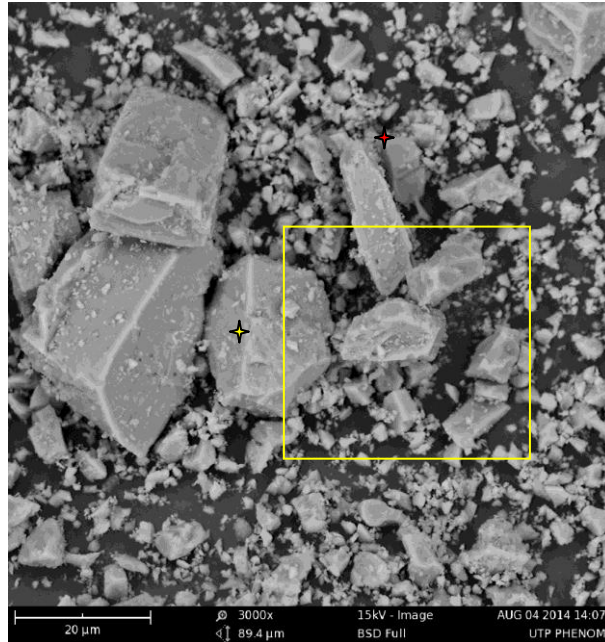


Figure 59: The SEM photo and EDS spots and map of facies RU1

The above figures show the SEM pictures under magnification of 3000 with a scale of 20 μm of RU1 samples. The sample is limestone. The large crystal is identified as dolomite. For further confirmation of the dolomite present, the energy-dispersive X-ray spectroscopy, also known as EDS is used on the sample represented by two star spots and a square. The EDS analyses are shown as follow:

Sample of RU1 (EDS)

Spot No. 1 (Yellow star)

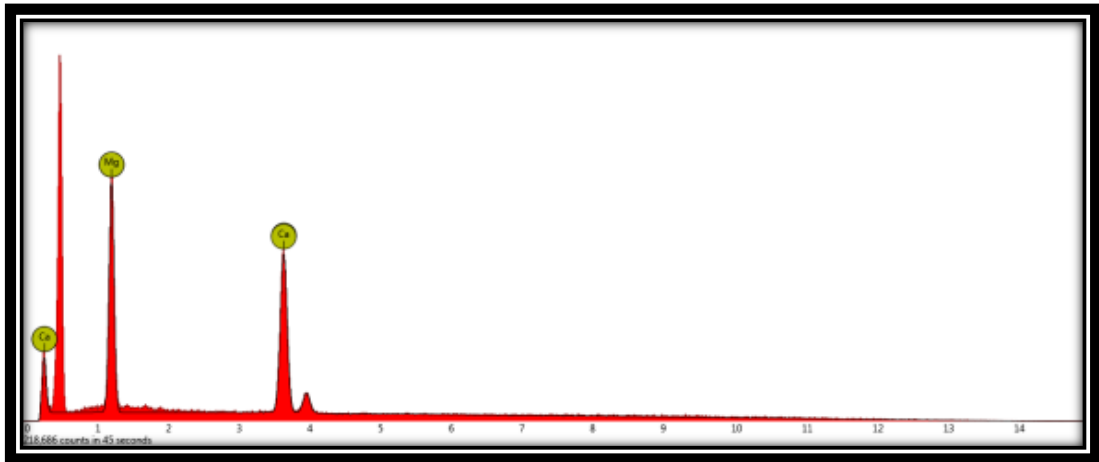


Figure 60: EDS graph of facies Ru1 at spot 1 (red star)

Table 21 Table of EDS analysis of facies RU1

Element Number	Element Symbol	Element Name	Confidence	Concentration	Error
12	Mg	Magnesium	100.0	60.7	0.7
20	Ca	Calcium	100.0	39.3	0.7

Spot No. 2 (Red star)

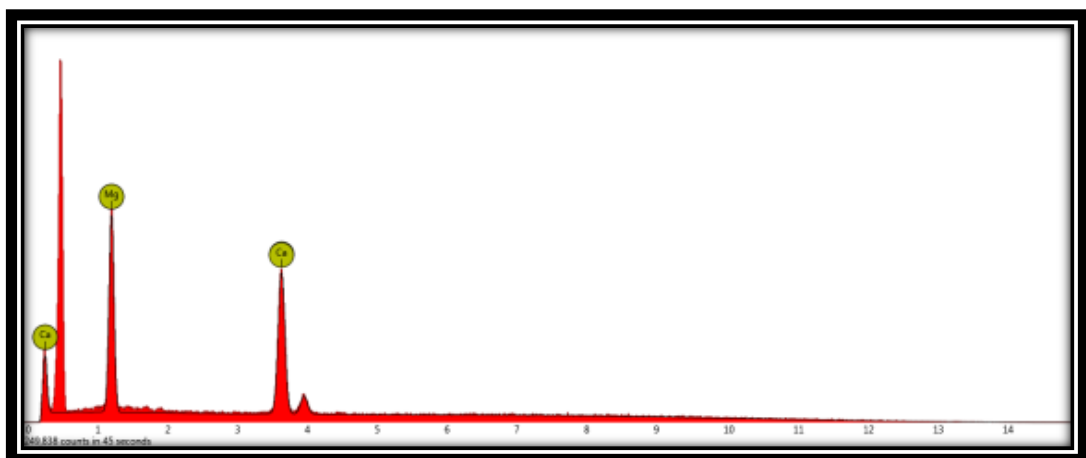


Figure 61: EDS graph of facies RU1 at yellow spot 2

Table 22 Table of EDS analysis of facies RU1

Element Number	Element Symbol	Element Name	Confidence	Concentration	Error
12	Mg	Magnesium	100.0	60.1	0.7
20	Ca	Calcium	100.0	39.9	0.7

Map (Yellow square)

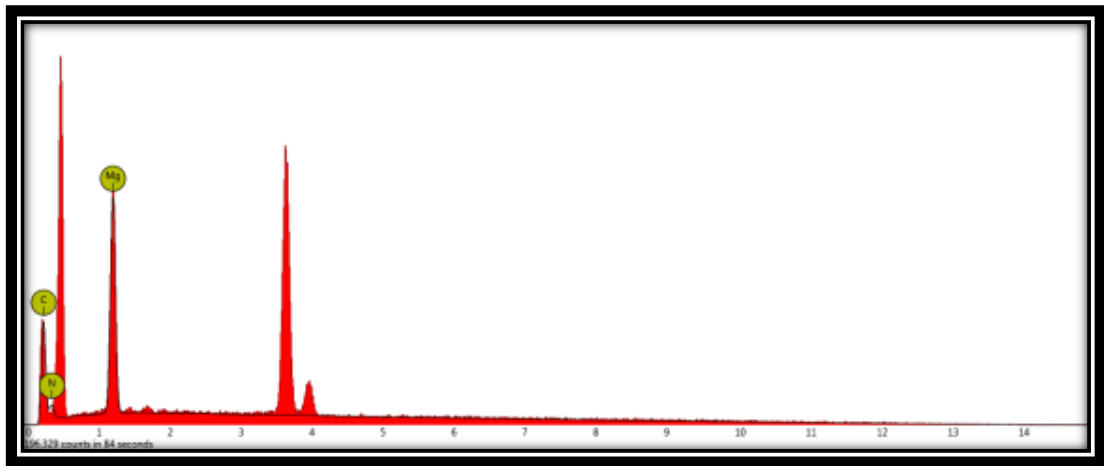


Figure 62: EDS graph of facies RU1 in yellow square map

Table 23 Table of EDS of facies RU1 in yellow square map

Element Number	Element Symbol	Element Name	Confidence	Concentration	Error
12	Mg	Magnesium	100.0	52.3	0.8
6	C	Carbon	100.0	28.0	1.3
7	N	Nitrogen	100.0	19.7	4.5

From the above three EDS graph shows peaks caused by energy of the X-ray emitted from the sample; a high-energy beam of charged particles or an X-rays beam, is focused into the studied sample. Thus, the number and the energy of the emitted X-rays from a sample can be measured by an-energy dispersive spectrometer. The EDS

results are shown in the above three table. From the results, element of magnesium and calcium are constantly identified from the sample and these two elements is the basic chemical compositions of dolomite ($\text{MgCa}(\text{CO}_3)_2$). In conclusion, SEM and EDS results are tallied to each other and hence, confirmed the present of dolomite. The other three results of RU2, RU3 and RU4 are also shown composition of predominantly of magnesium and calcium which the present of dolomite is affirmative in four samples tested using SEM and EDS. The results of RU2, RU3 and RU4 are attached in Appendix.

CHAPTER 5

CONCLUSION AND RECOMMENDATION

In conclusion based on the conducted study in the quarry area at the northern part of Sungai Siput, Perak in term of general geology, the limestone hills are surrounded by alluvium which the alluvium is overlies the carbonate rock body. The features of limestone hills are the remaining exposed carbonate rock and karstic. There are seven slightly different facies observed at the limestone hill. In the eastern direction from the limestone hills, a granite body is present which a part of the Main Range of Titiwangsa. However, the limestone hill has not been metamorphosed and changed to marble or dolostone. One of the hypotheses that can be concluded that, the limestone hills at the northern part of Sungai Siput, Perak is once at the top of the granite and further from the source of temperature and pressure to make the limestone to metamorphose. In time, the overlying limestone above the granite body was slightly moved downwards due to the fault or fractures system at the contacts of the limestone and granite. The fractures at the area are concentrated towards south-east direction based on the stereonet analysis.

FTIR, XRD, SEM and EDS showed constant results to confirm the presence of dolomite. The presence of dolomite indicated that the limestone hills had undergone dolomitization where the magnesium replaces calcite minerals. From the FTIR results, it has shown the presence of dolomite as mineral composition and the presence of magnesium as chemical composition. The XRD results provided strong evidences the presence of chemical composition of dolomite where the generated graphs of XRD are matched with EVA database. Furthermore, EDS showed

chemical composition of magnesium and calcium in four tested samples. Thus, the presence of dolomite is strongly confirmed by the analytical analyses and the limestone hills in the quarry area are confirmed to have undergone dolomitization.

Recommendation: The study is conducted in a longer period where more samples and more locations can be studied. The research can be studied in terms of the degree of dolomitization either laterally or vertically of the limestone hills.

REFERENCES

- Abd Kadir, A., Pierson, B., Tuan Harith, Z. Z. and Weng Sum, C. 2008. Paleozoic limestone of the Kinta Valley: Paleogeography and implications to the regional geology of Peninsular Malaysia - UTP Institutional Repository. [online] Available at: <http://eprints.utp.edu.my/5556/> [Accessed: 19 Feb 2014].
- Boon Kong, T. 2014. Engineering Geology of Limestone in Malaysia. *Acta Geologica Sinica – English Edition*, 75 (3), pp. 54-56. Available from: doi: 10.1111/j.1755-6724.2001.tb00538.x.
- Coates, J., 2000. Interpretation of Infrared Spectra, A Practical Approach. *Encyclopedia of Analytical Chemistry*, R.A. Meyers (Ed.), pp. 10815-10837.
- Huang, C.K. & Kerr, P.F. (1960). Infrared Study of the Carbonate Minerals. *The American Mineralogist*, Vol. 45, March-April 1960.
- Ingham, F. T. & Bradford, E. F. 1960. The geology and mineral resources of the Kinta Valley, Perak. *Geological Survey Federated Malaya* 9.
- Islahuda Hani Sahak, MohdShafeea Leman, RosFatimah Muhammad & MohdIrwanAriff 2009. Potensi pembangunan lestari sumber geowarisan Lembah Kinta. In Che Aziz Ali, MohdShafeea Leman, Kamal Roslan Mohamed & Ibrahim Komoo (eds.) *Geological Heritage of Malaysia – Towards Proclaiming Geoheritage Resources*. Lestari UKM Publications, Bangi, 216-240.
- Land, L.S., 1986. Limestone diagenesis—some geochemical considerations. In: Mumpton, F.A. (Ed.), *Studies in Diagenesis*. Washington. US Geol. Surv. Bull. 1578, pp. 129–137.
- Martinek, K. (n.d.). *Carbonates II: Diagenesis, Dolomitization. Petrology of Sedimentary Rocks*. Institute of Geology and Palentology.
- Moore, C.H. (1989). *Carbonate diagenesis and Porosity. Developments in Sedimentology*, pp. 46. Elsevier.
- Moore, C.H., 2001. *Carbonate Reservoirs: Porosity Evolution and Diagenesis in a Sequence Stratigraphic Framework. Developments in Sedimentology*. Elsevier, Amsterdam, p. 444.
- Peters, K. E., Walters, C.C. and Moldowan, J.M (2005) *The Biomarker Guide Volume 1: Biomarkers and Isotopes in the environment and Human History*, Cambridge University Press

- Raj, J.K., Tan, D. N. K. & Wan Hasiah Abdullah 2009. Cenozoic Stratigraphy. In Hutchison, C. S. & Tan, D. N. K. (eds.) Geology of Peninsular Malaysia. Universiti Malaya and Geological Society of Malaysia Publication, Kuala Lumpur, 133-173.
- RosFatimah Muhammad & Ibrahim Komoo 2003. The Kinta Valley karst landscape – a national heritage to be preserved. Geological Society of Malaysia Bulletin 46, 447-453.

APPENDICES

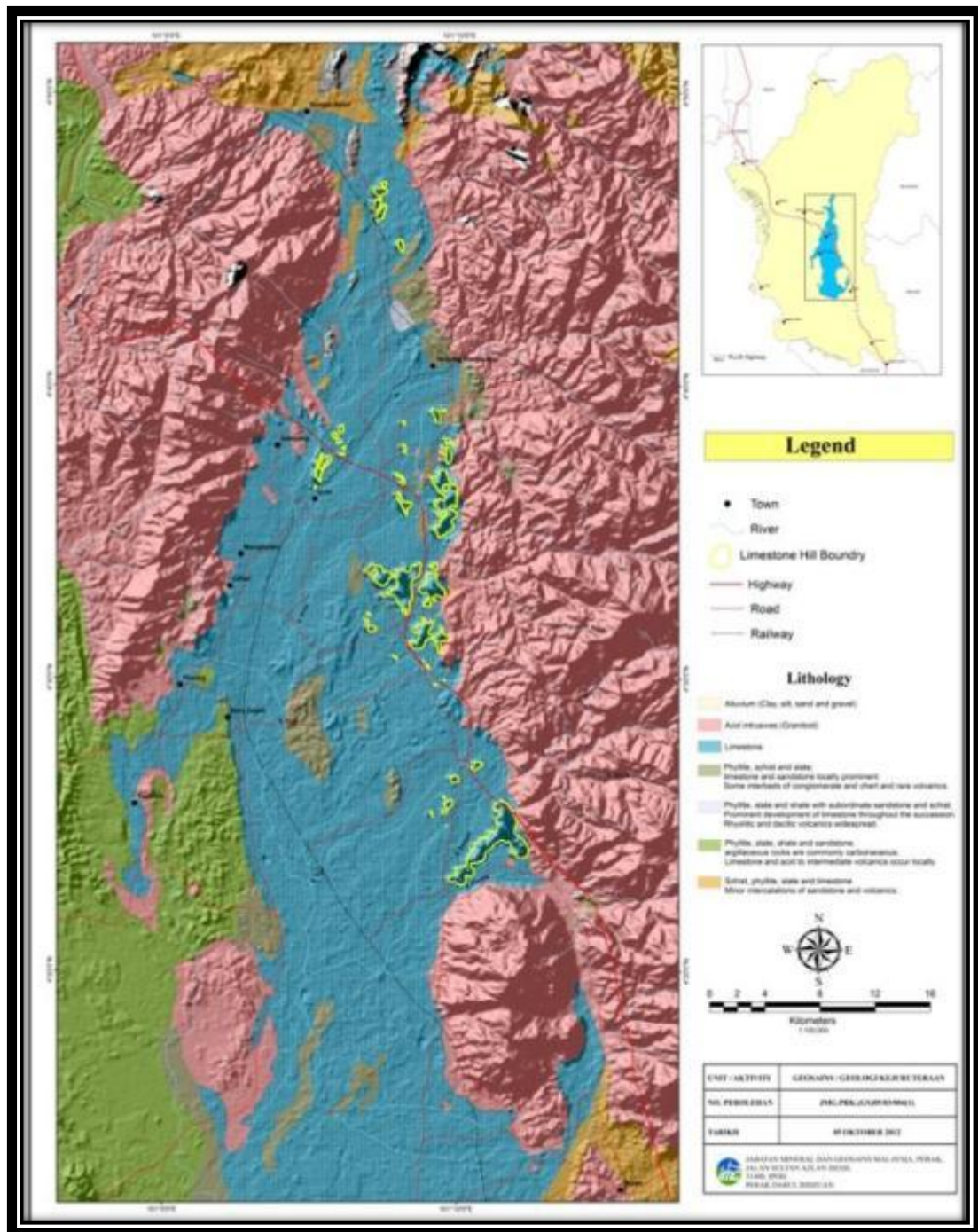


Figure 63: The geological map of Kinta Valley (Jabatan Mineral dan Geosains Malaysia, 2009)

Fourier Transform Infrared Spectroscopy (FTIR)

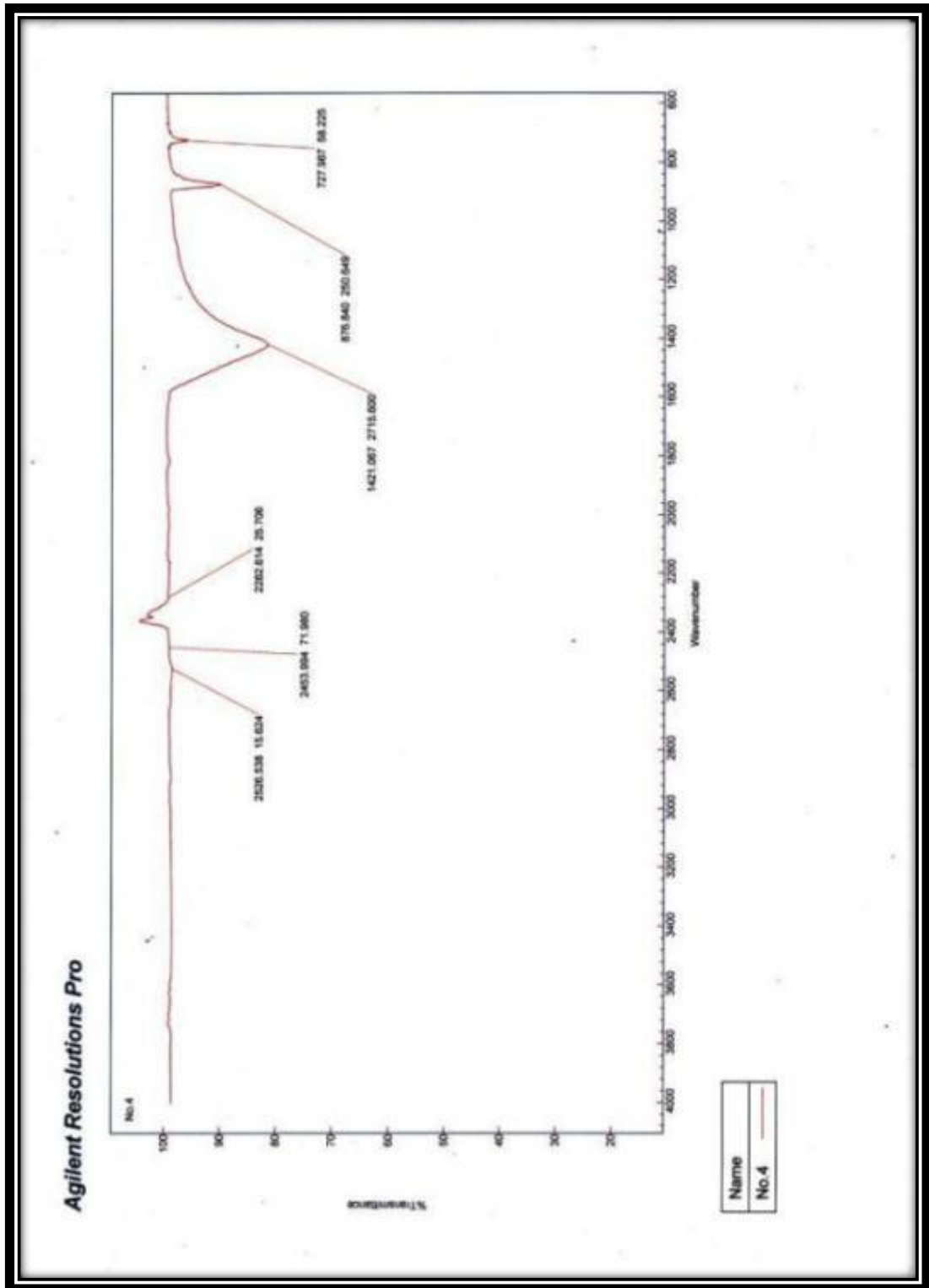


Figure 64: FTIR graph of facies N4

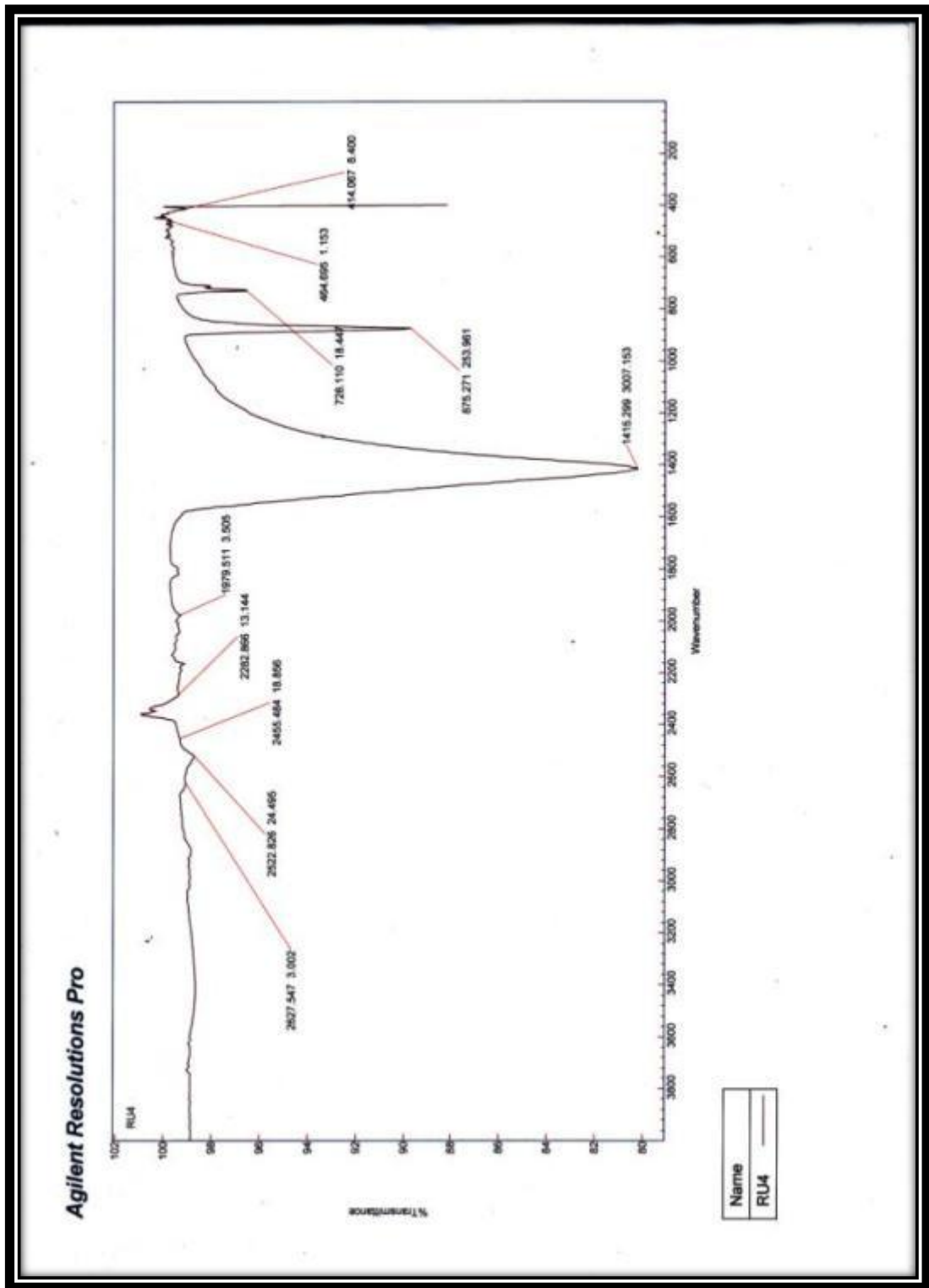


Figure 65: FTIR graph of facies RU4

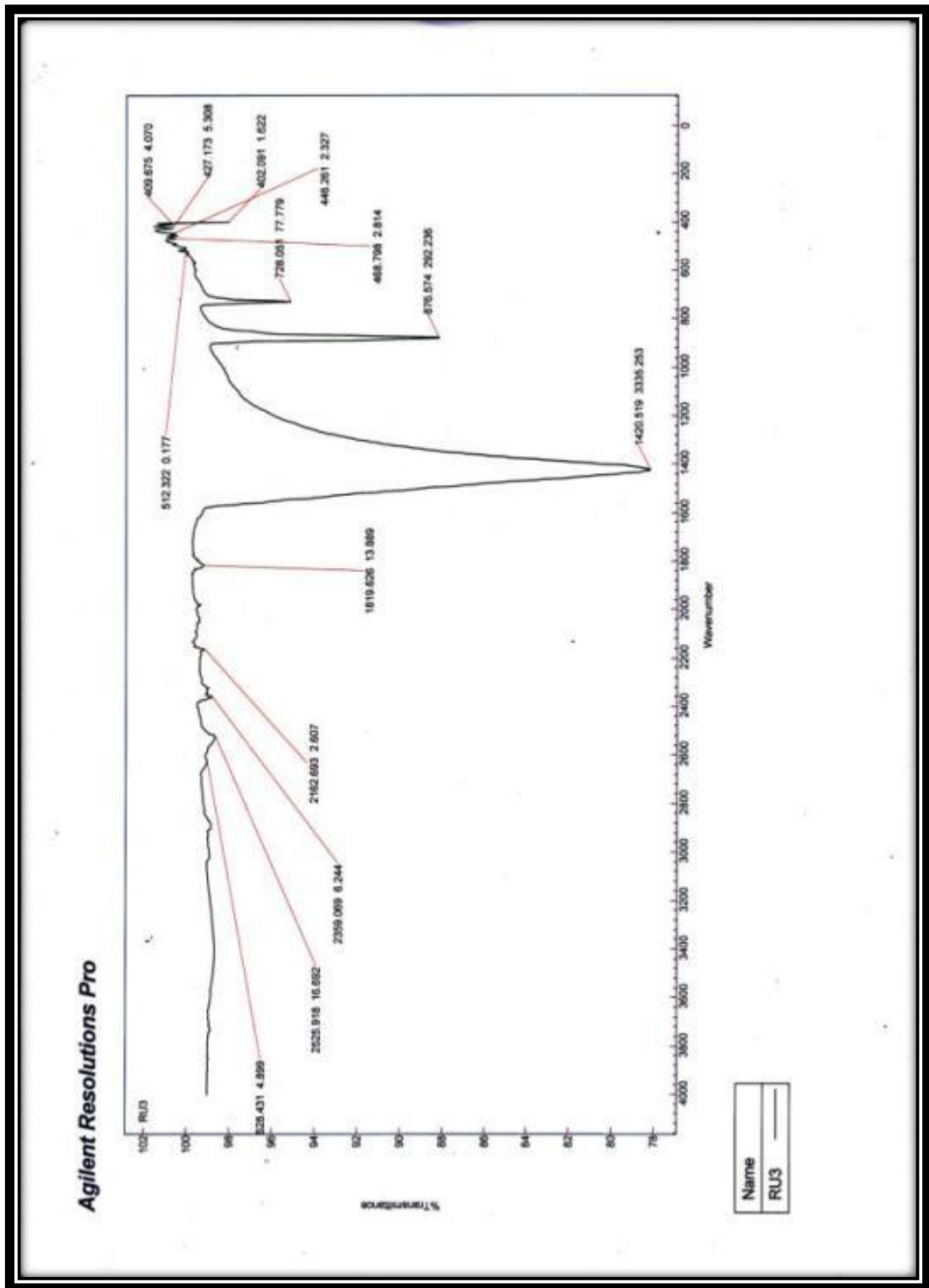


Figure 67: FTIR graph of facies RU3

Thin Section

Sample 1 (4x)

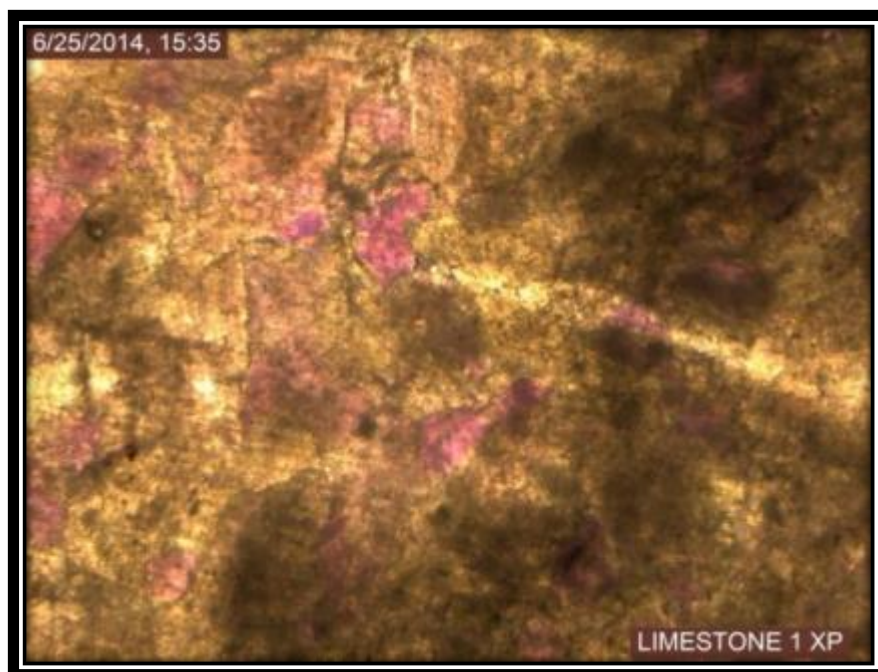
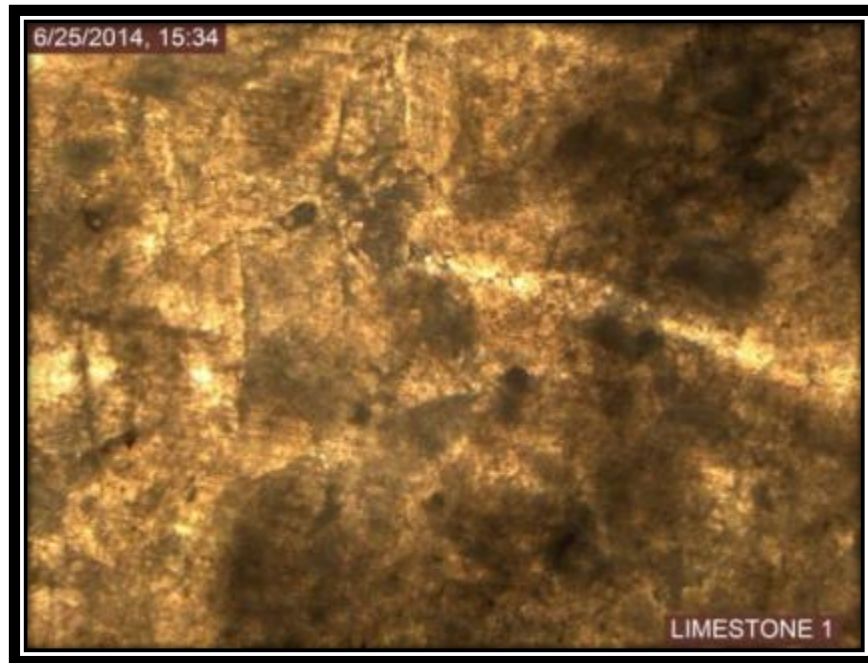


Figure 68: Thin section of sample 1(Magnification: 4x)

Sample 2 (10x)



Figure 69: Thin section of sample 2 (Magnification: 10x)

Sample 3 (4x)

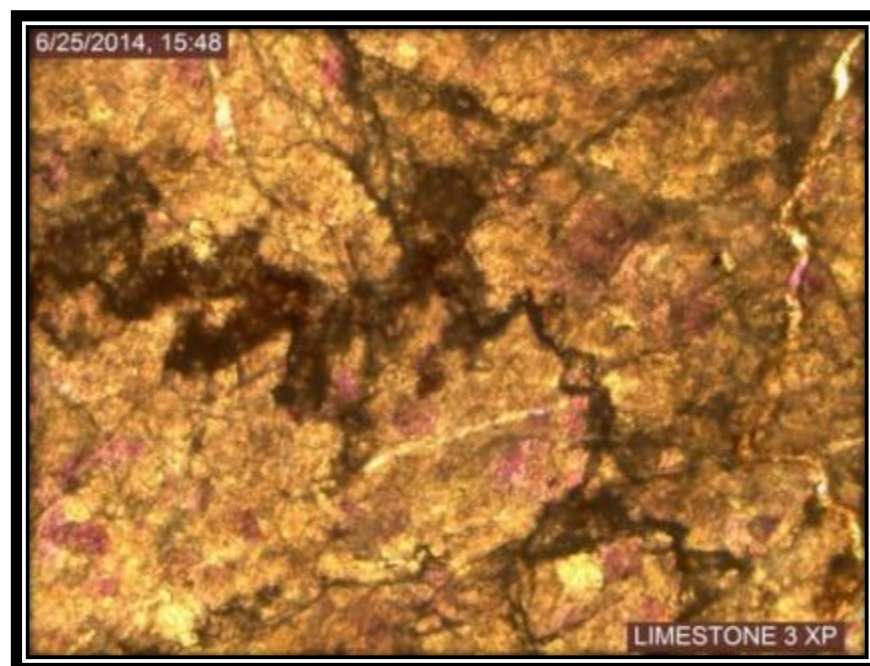
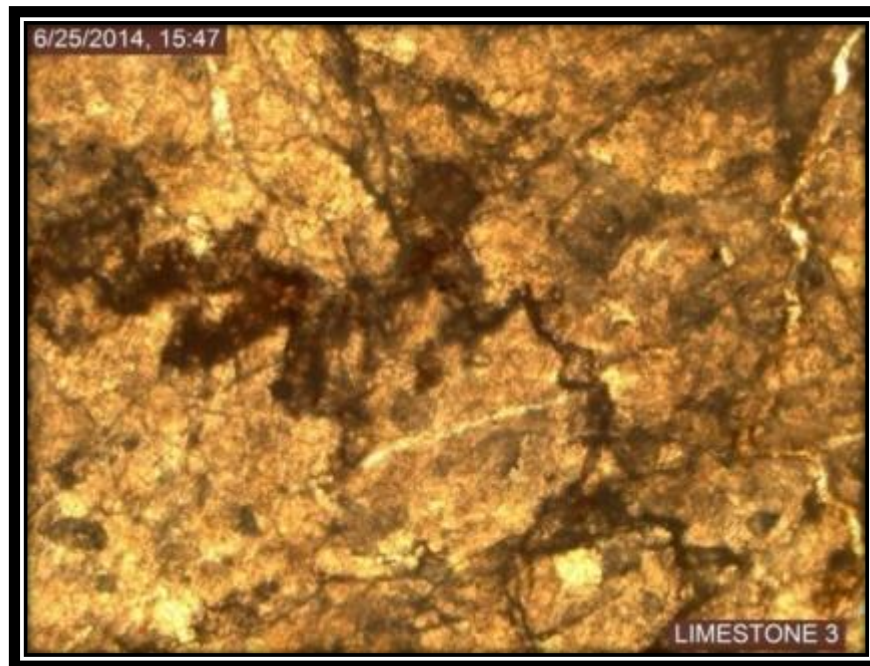


Figure 70: Thin section of sample 3 (Magnification: 4x)

Sample 4 (4x)

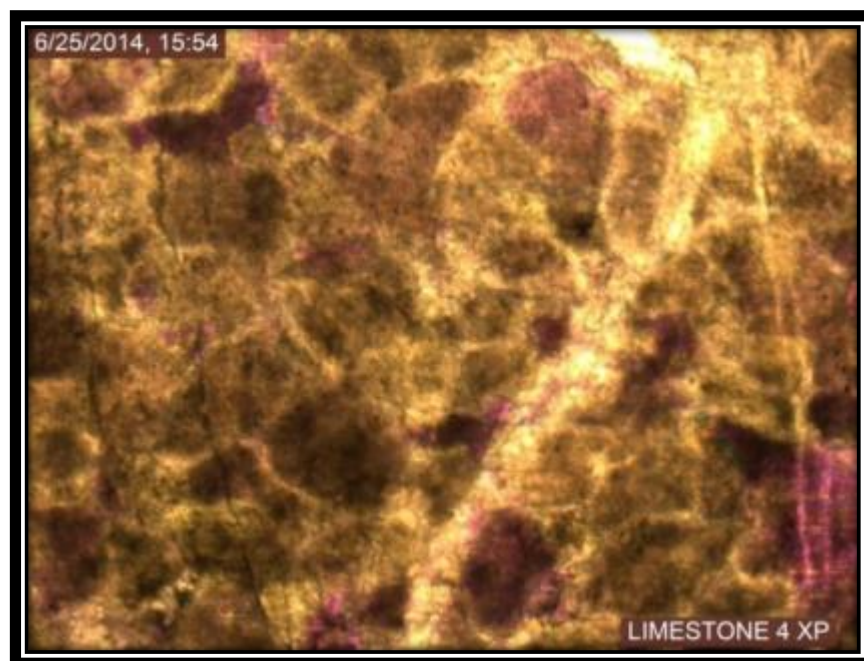
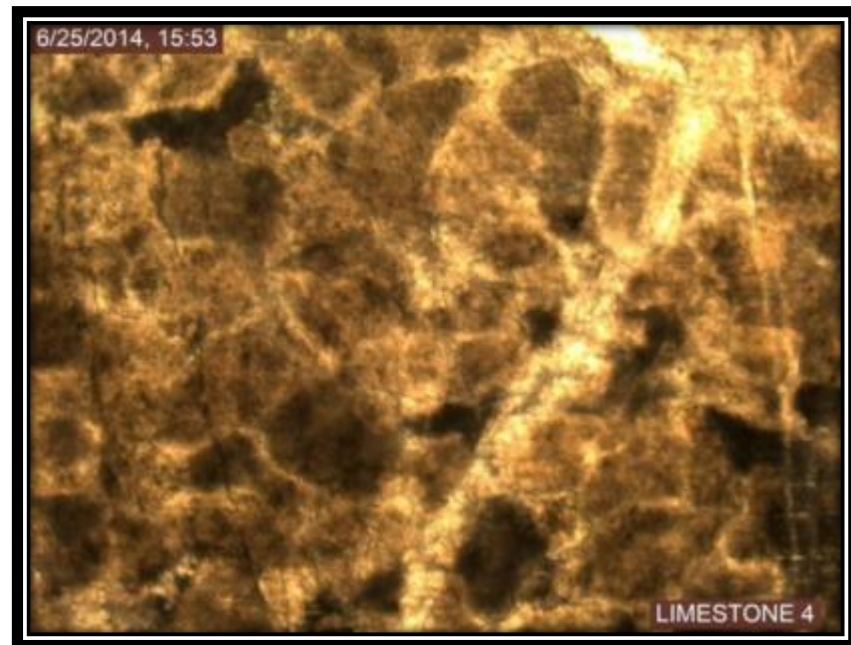


Figure 71: Thin section of sample 4 (Magnification: 4x)

Sample 9 (4x)

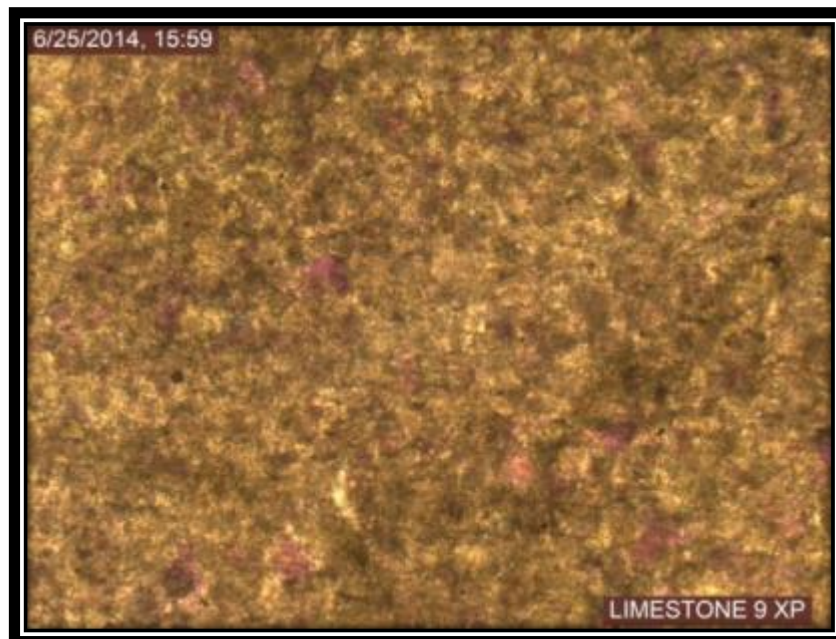
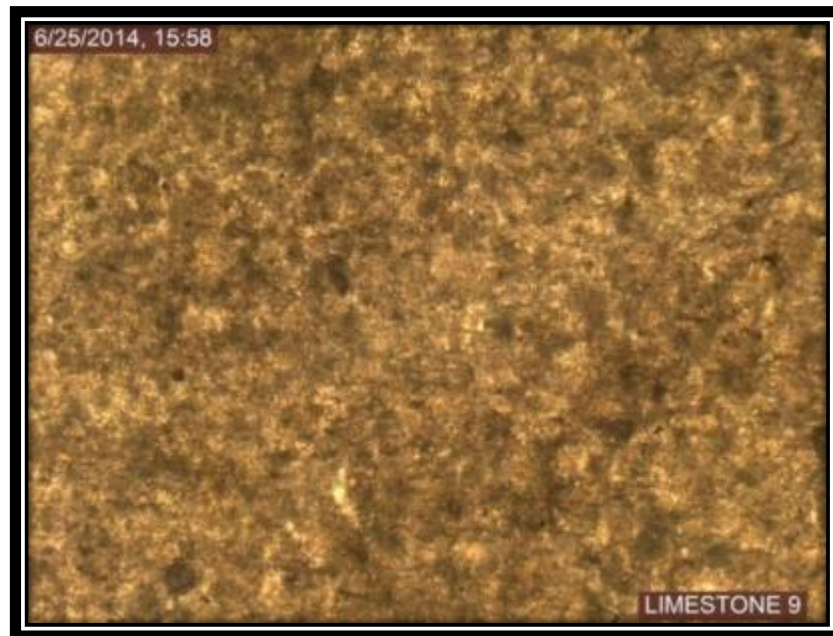


Figure 72: Thin section of sample 9 (Magnification: 4x)

Sample 11 (4x)

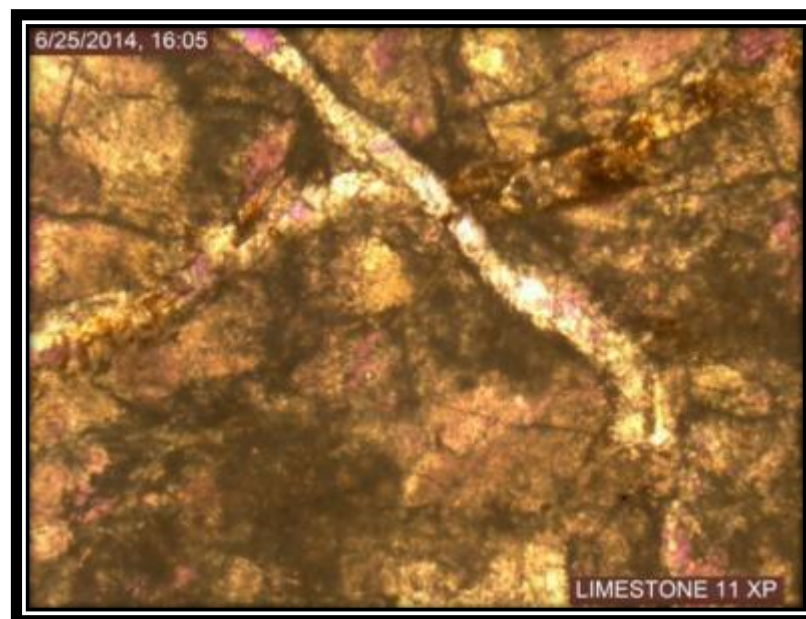
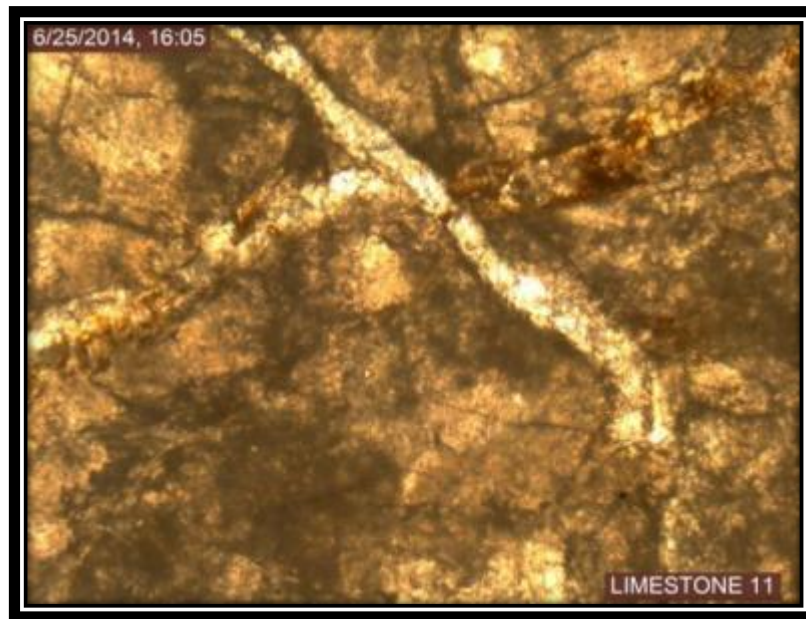


Figure 73: Thin section of sample 11 (Magnification: 4x)

Total Carbon

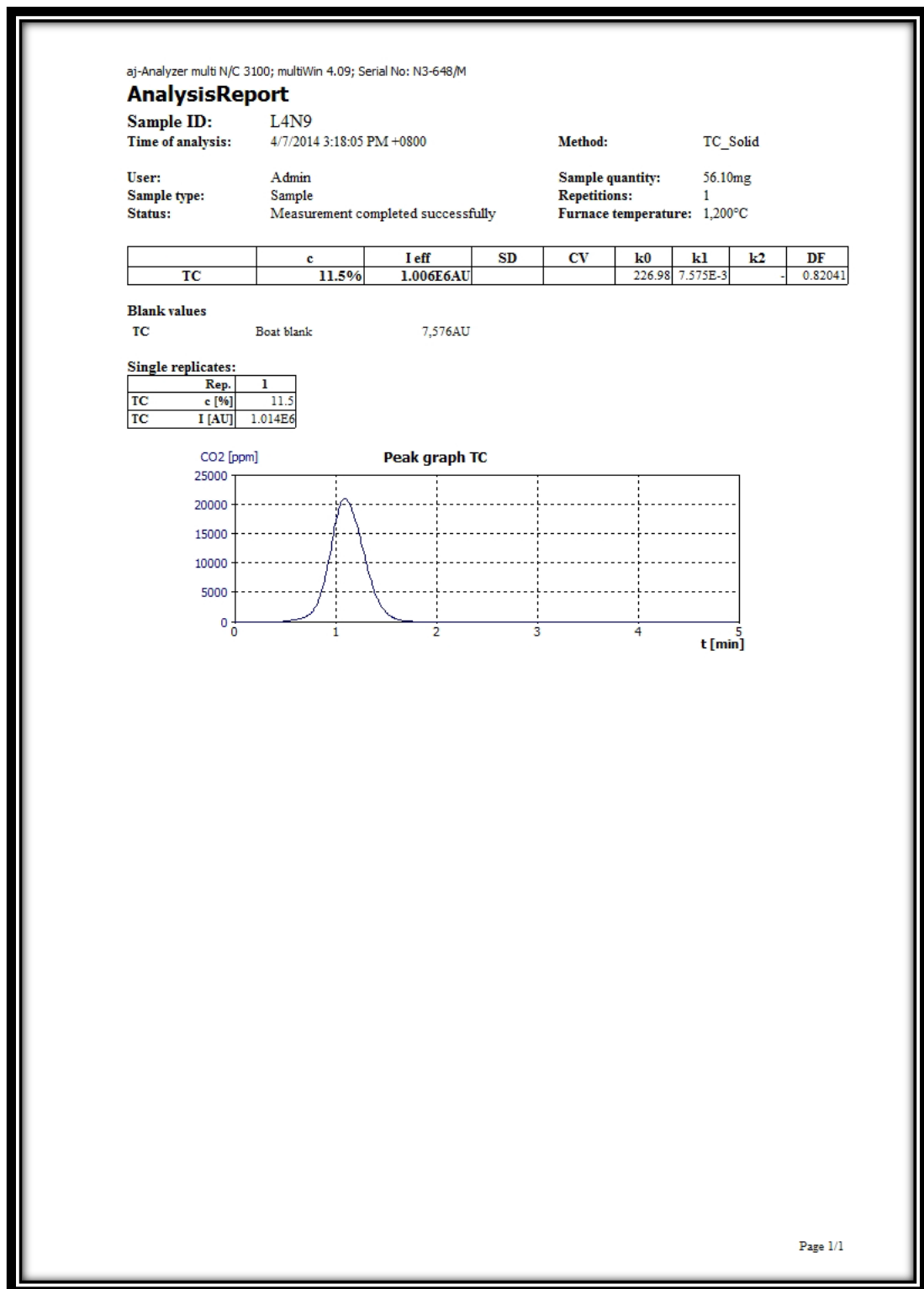


Figure 74: Analysis Report of Total Carbon of L4

Analysis Report

Sample ID: No4
Time of analysis: 4/7/2014 4:08:31 PM +0800
Method: TC_Solid
User: Admin
Sample type: Sample
Status: Measurement completed successfully
Sample quantity: 56.60mg
Repetitions: 1
Furnace temperature: 1,200°C

	c	I eff	SD	CV	k0	k1	k2	DF
TC	12.1%	1.07E6AU			226.98	7.575E-3	-	0.82041

Blank values

TC Boat blank 7,576AU

Single replicates:

Rep.	1
TC c [%]	12.1
TC I [AU]	1.078E6

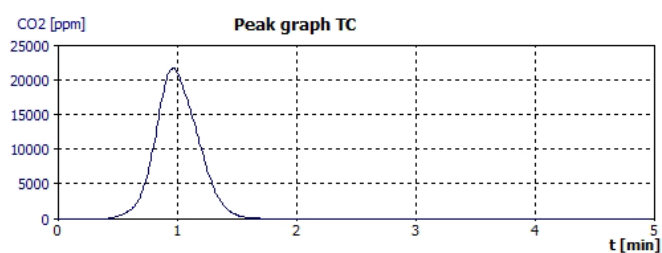


Figure 75: Analysis Report of Total Carbon of N4

Analysis Report

Sample ID: R1NO1
Time of analysis: 4/7/2014 3:52:48 PM +0800
Method: TC_Solid
User: Admin
Sample type: Sample
Status: Measurement completed successfully
Sample quantity: 59.30mg
Repetitions: 1
Furnace temperature: 1,200°C

	c	I eff	SD	CV	k0	k1	k2	DF
TC	11.4%	1.062E6AU			226.98	7.575E-3	-	0.82041

Blank values

TC Boat blank 7,576AU

Single replicates:

	Rep.	1
TC	c [%]	11.4
TC	I [AU]	1.069E6

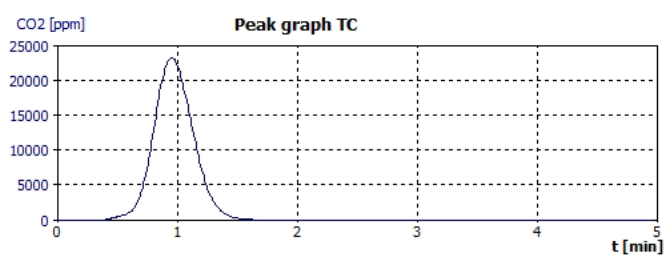


Figure 76: Analysis Report of Total Carbon of RU1

Analysis Report

Sample ID: R4_no11
Time of analysis: 4/7/2014 4:23:26 PM +0800
Method: TC_Solid
User: Admin
Sample type: Sample
Status: Measurement completed successfully
Sample quantity: 55.80mg
Repetitions: 1
Furnace temperature: 1,200°C

	c	I eff	SD	CV	k0	k1	k2	DF
TC	11.9%	1.042E6AU			226.98	7.575E-3	-	0.82041

Blank values

TC Boat blank 7,576AU

Single replicates:

Rep.	1
TC	c [%] 11.9
TC	I [AU] 1.049E6

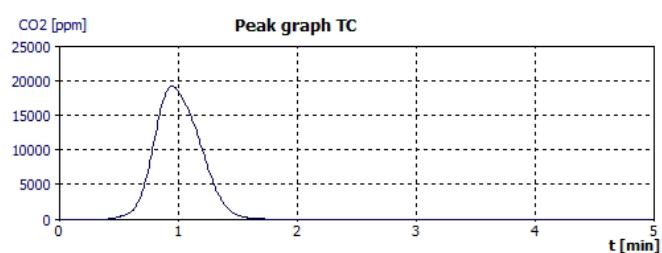


Figure 77: Analysis Report of Total Carbon of RU4

aj-Analyzer multi N/C 3100; multiWin 4.09; Serial No: N3-648/M

Analysis Report

Sample ID: RO2
Time of analysis: 4/7/2014 4:00:24 PM +0800
Method: TC_Solid

User: Admin
Sample type: Sample
Status: Measurement completed successfully

Sample quantity: 55.60mg
Repetitions: 1
Furnace temperature: 1,200°C

	c	I eff	SD	CV	k0	k1	k2	DF
TC	12.3%	1.074E6AU			226.98	7.575E-3	-	0.82041

Blank values

TC Boat blank 7,576AU

Single replicates:

Rep.	1
TC	c [%] 12.3
TC	I [AU] 1.082E6

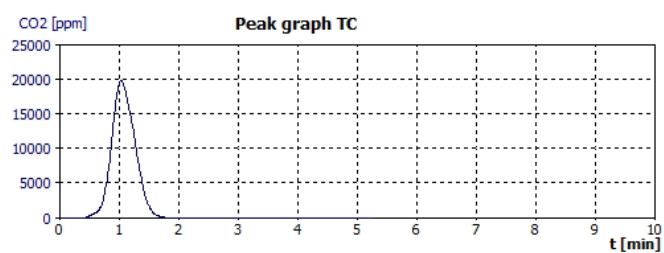


Figure 78: Analysis Report of Total Carbon of RU2

aj-Analyzer multi N/C 3100; multiWin 4.09; Serial No: N3-648/M

AnalysisReport

Sample ID: RU3
Time of analysis: 4/7/2014 4:18:34 PM +0800
Method: TC_Solid
User: Admin
Sample type: Sample
Status: Measurement completed successfully
Sample quantity: 56.30mg
Repetitions: 1
Furnace temperature: 1,200°C

	c	I eff	SD	CV	k0	k1	k2	DF
TC	11.1%	9.752E5AU			226.98	7.575E-3	-	0.82041

Blank values

TC Boat blank 7,576AU

Single replicates:

Rep.	1
TC c [%]	11.1
TC I [AU]	9.828E5

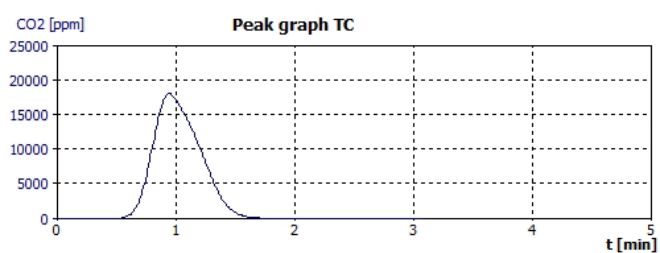


Figure 79: Analysis Report of Total Carbon of RU3

X-ray Diffraction (XRD)

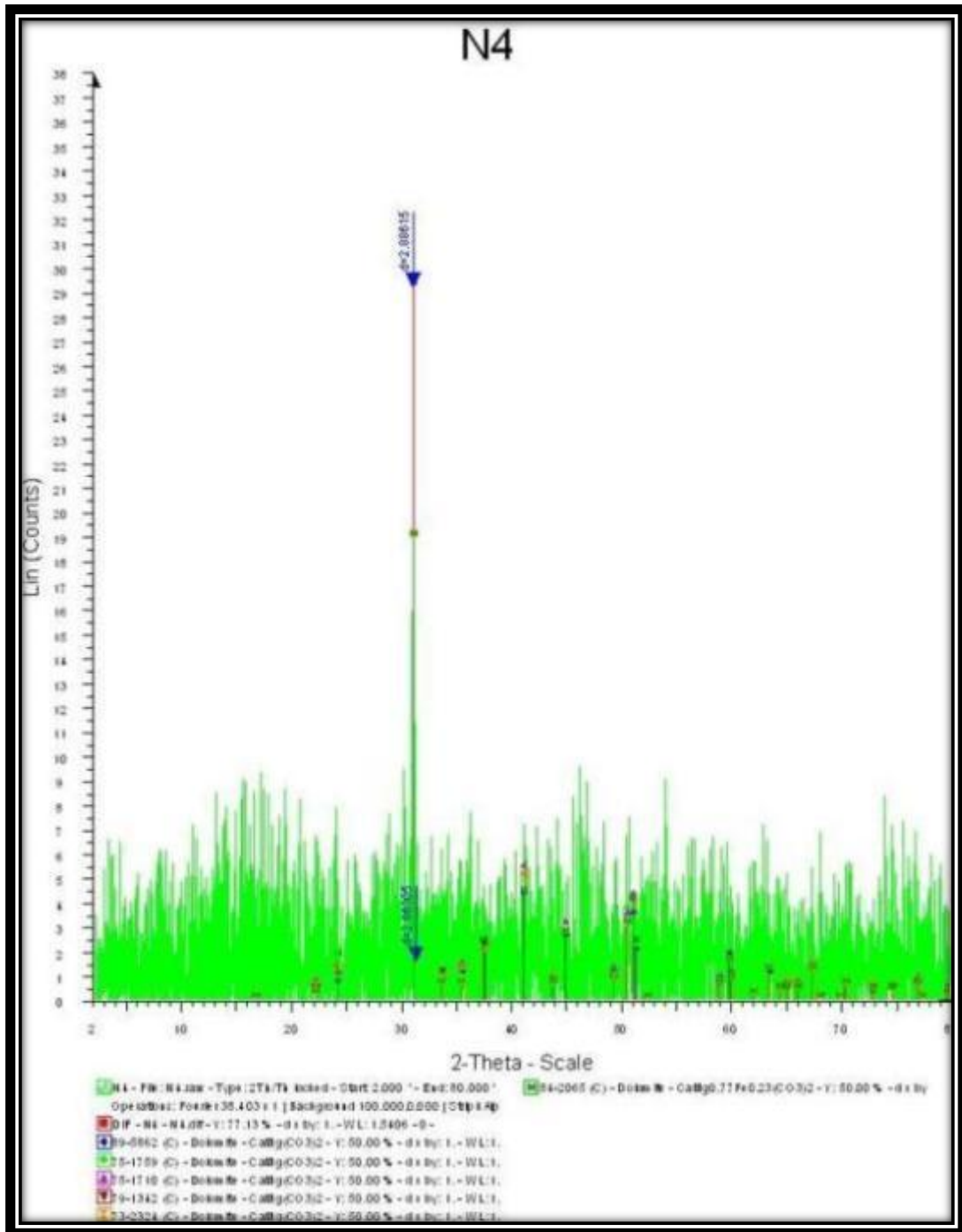


Figure 80: XRD result of N4

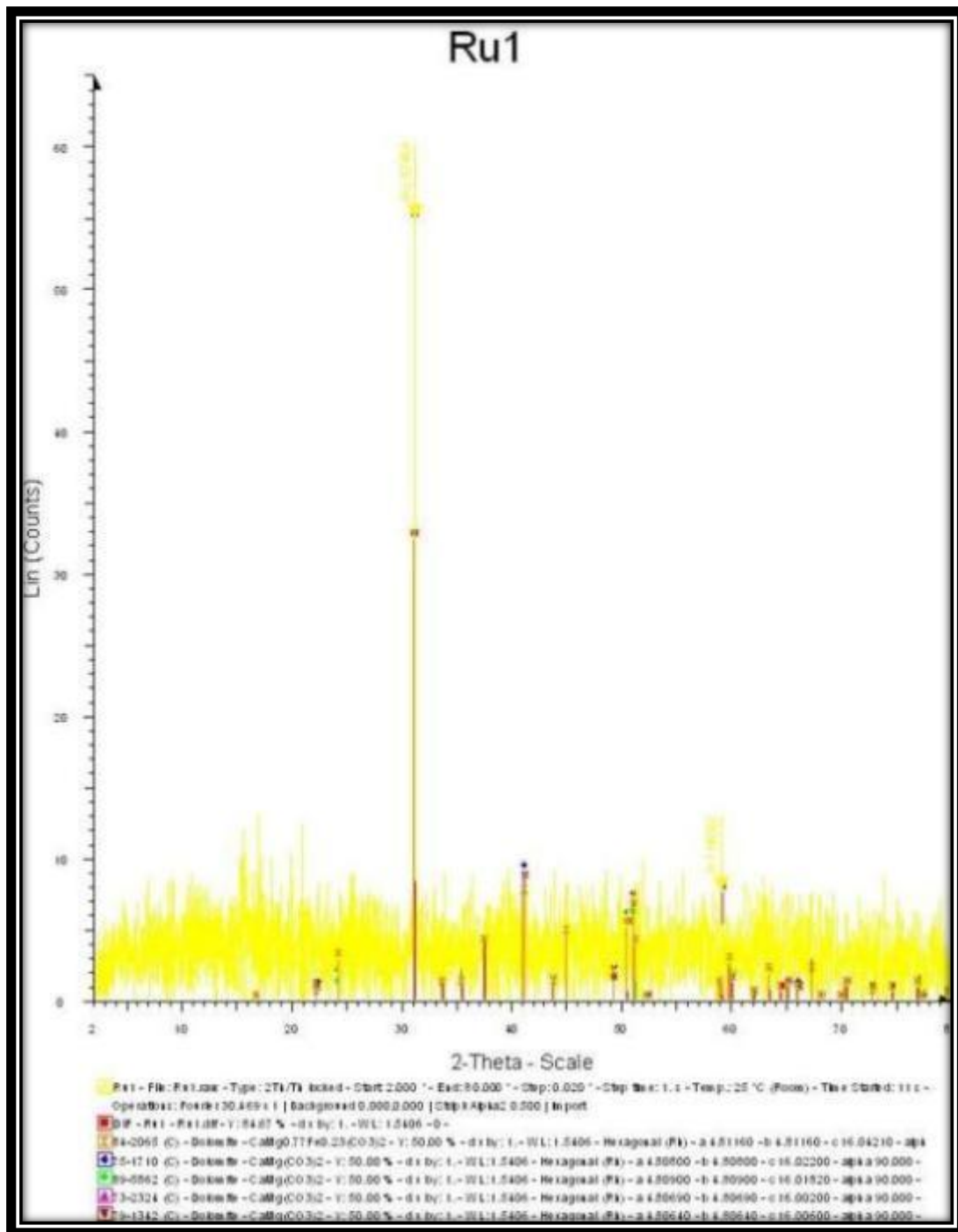


Figure 81: XRD result of RU1

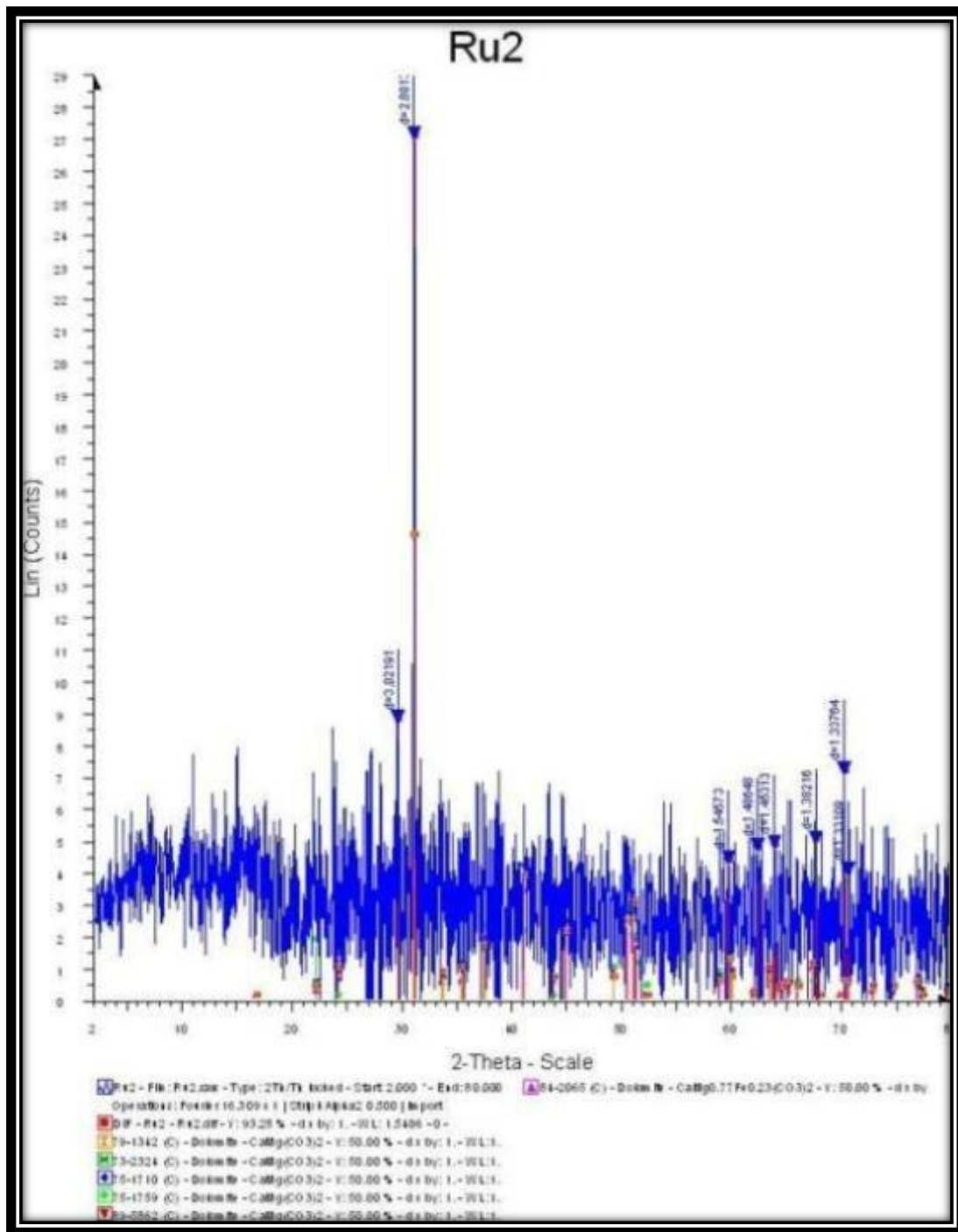


Figure 82: XRD result of RU2

Scanning electron microscopy (SEM) and Energy-dispersive X-ray spectroscopy (EDS)

RU2 SEM

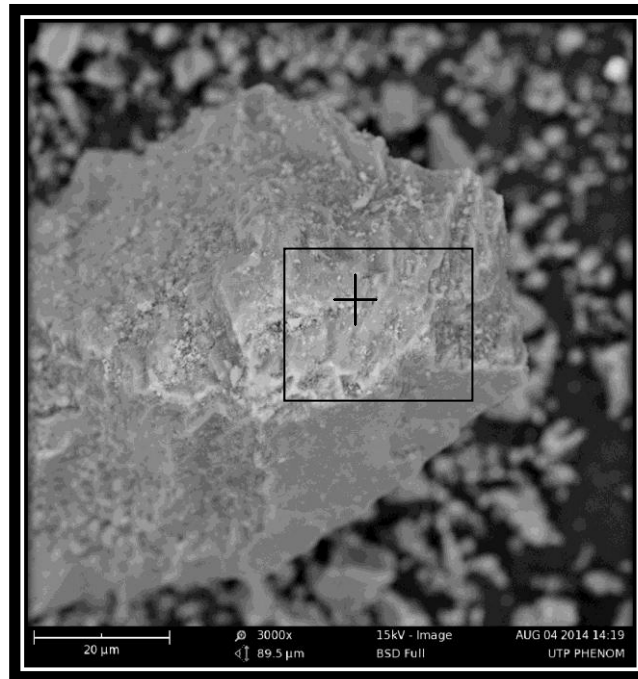


Figure 83: SEM and EDS photo with spot and map EDS analysis of RU2

R_2 EDS

Spot

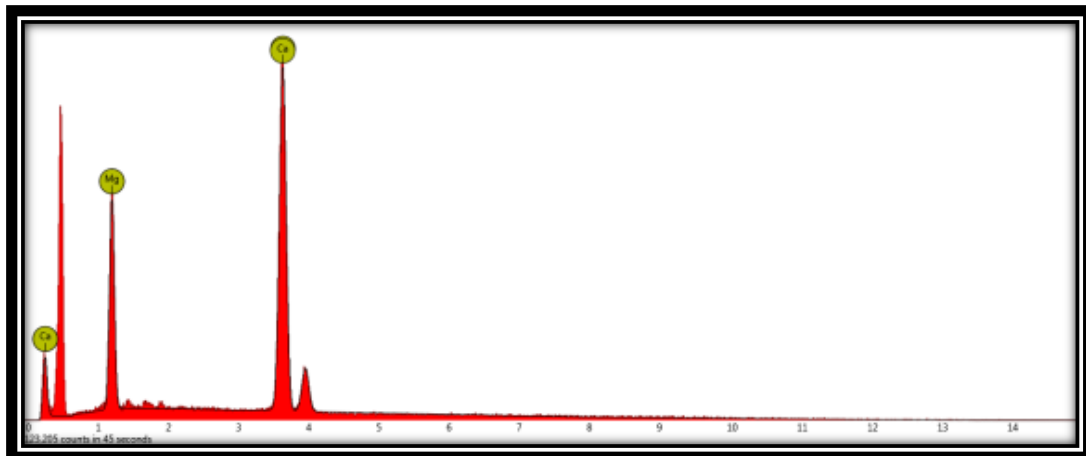


Figure 84: EDS graph of facies RU2 at spot

Table 24 Table of EDS analysis of facies RU2 at the spot

Element Number	Element Symbol	Element Name	Confidence	Concentration	Error
20	Ca	Calcium	100.0	54.8	0.6
12	Mg	Magnesium	100.0	45.2	1.0

Square map

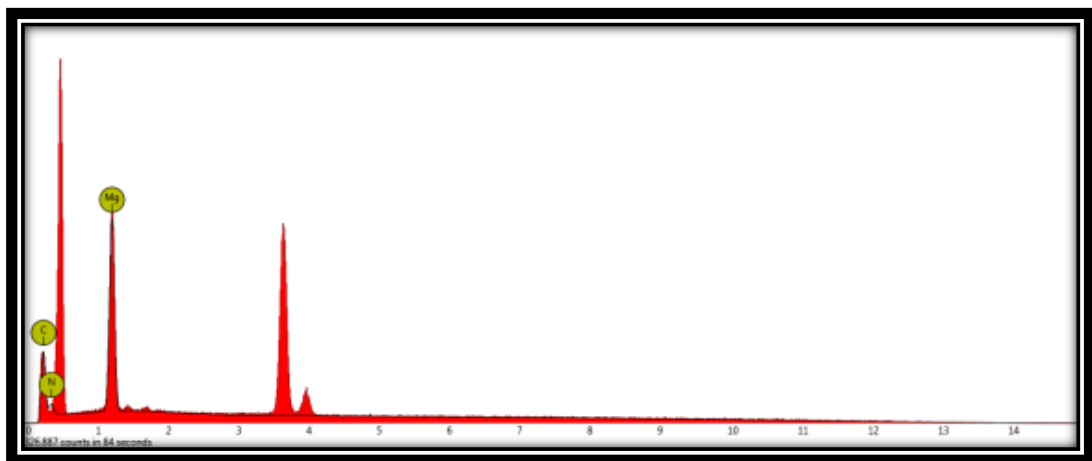


Figure 85: EDS graph of facies RU2 at map

Table 25 Table of EDS analysis of facies RU2 at map

Element Number	Element Symbol	Element Name	Confidence	Concentration	Error
12	Mg	Magnesium	100.0	56.6	0.6
6	C	Carbon	100.0	24.2	1.2
7	N	Nitrogen	100.0	19.2	4.0

RU3 SEM

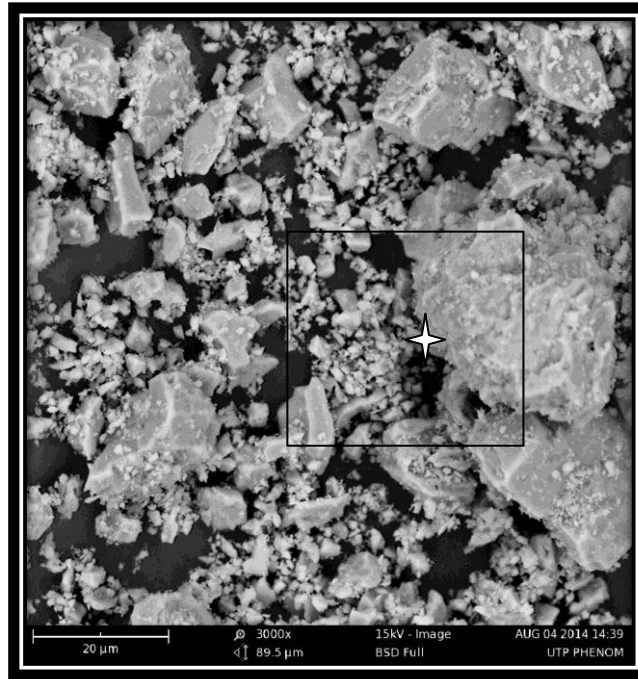


Figure 86: SEM and EDS photo with spot and map EDS analysis of RU3

R_3 EDS

White Spot

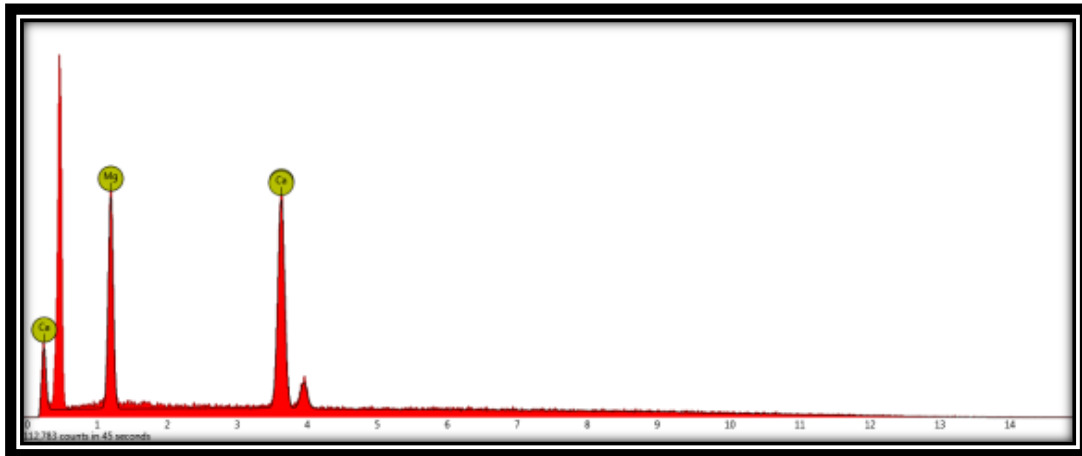


Figure 87: EDS graph of facies RU3 at white spot

Table 26 Table of EDS analysis of facies RU3 at white spot

Element Number	Element Symbol	Element Name	Confidence	Concentration	Error
12	Mg	Magnesium	100.0	54.5	1.0
20	Ca	Calcium	100.0	45.5	0.9

Square map

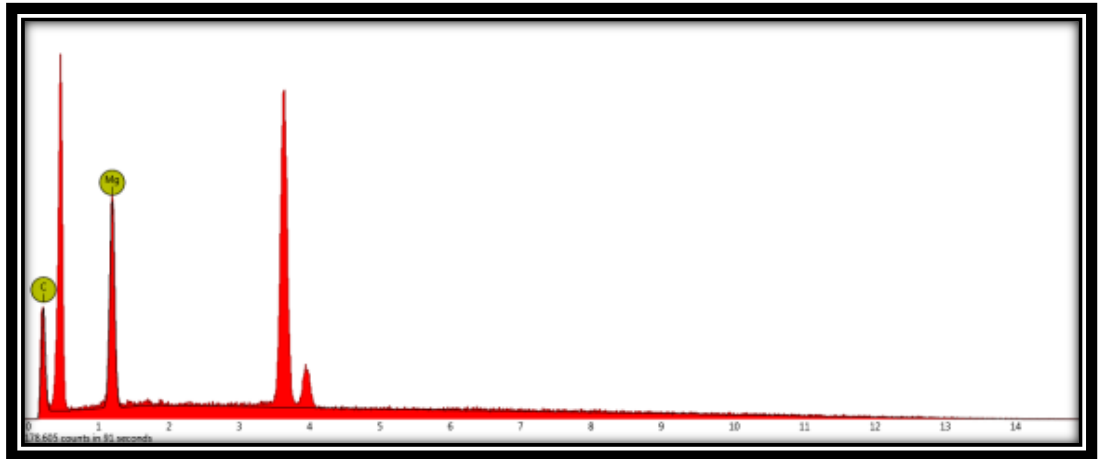


Figure 88: EDS graph of facies RU3 at square map

Table 27 Table of EDS analysis of facies RU3 at square map

Element Number	Element Symbol	Element Name	Confidence	Concentration	Error
12	Mg	Magnesium	100.0	57.8	0.9
6	C	Carbon	100.0	42.2	1.5

RU4 SEM

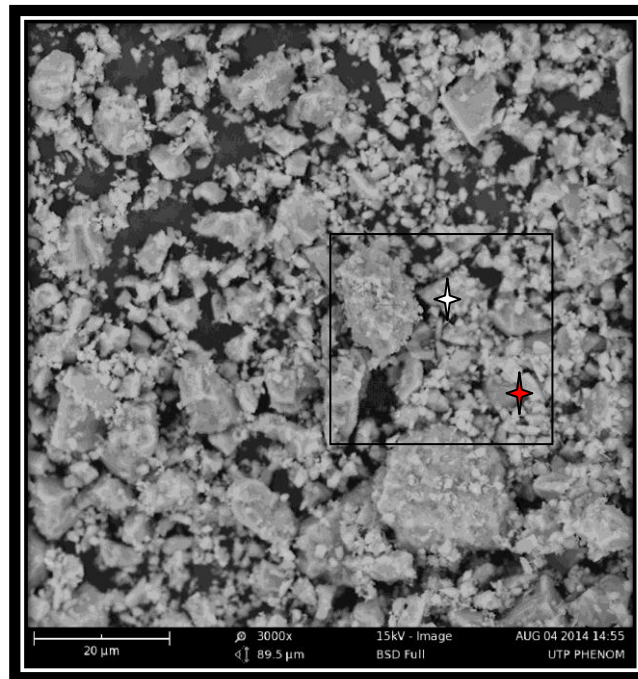


Figure 89: SEM and EDS photo with spot and map EDS analysis of RU4

R_4 EDS

White spot

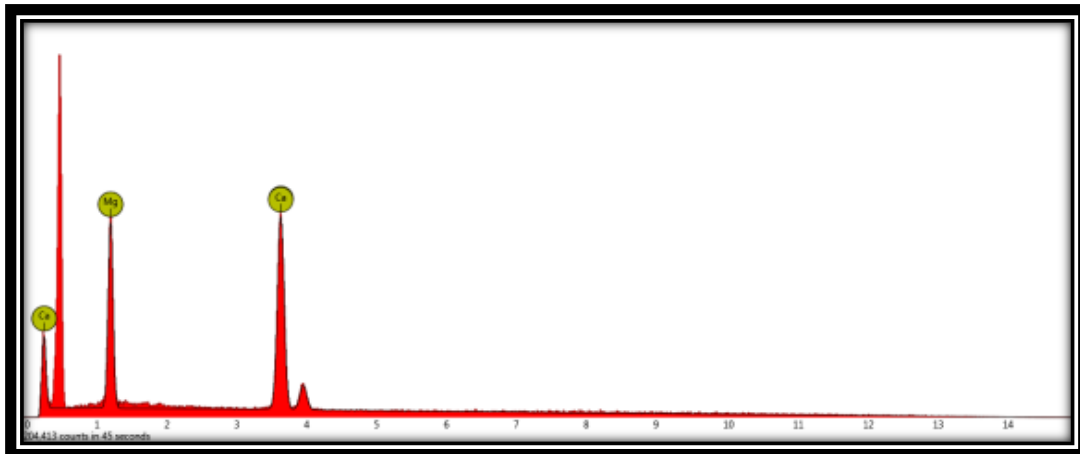


Figure 90: EDS graph of facies RU4 at white spot

Table 28 Table of EDS analysis of facies RU4 at white spot

Element Number	Element Symbol	Element Name	Confidence	Concentration	Error
20	Ca	Calcium	100.0	46.4	0.7
12	Mg	Magnesium	100.0	53.6	0.8

Red spot

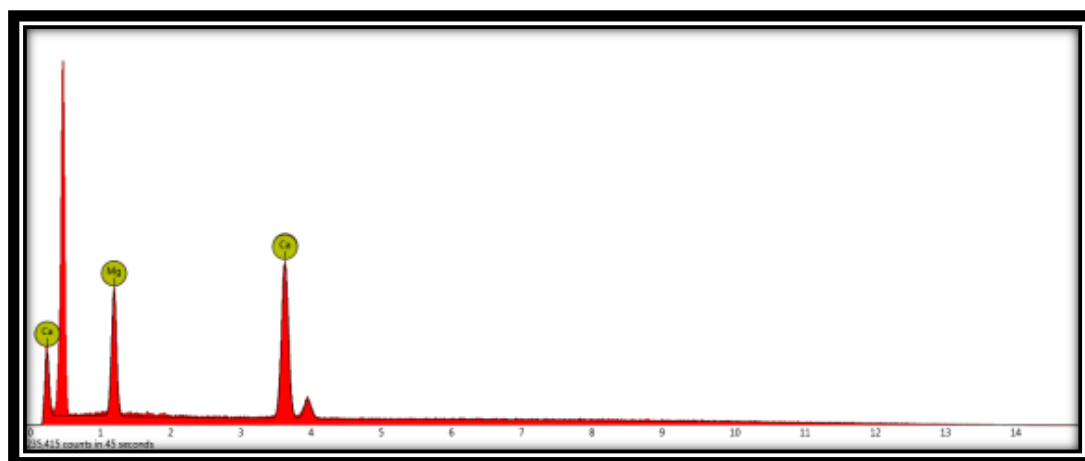


Figure 91: EDS graph of facies RU4 at red spot

Table 29 Table of EDS analysis of facies RU4 at red spot

Element Number	Element Symbol	Element Name	Confidence	Concentration	Error
20	Ca	Calcium	100.0	49.6	0.7
12	Mg	Magnesium	100.0	50.4	0.9

Square map

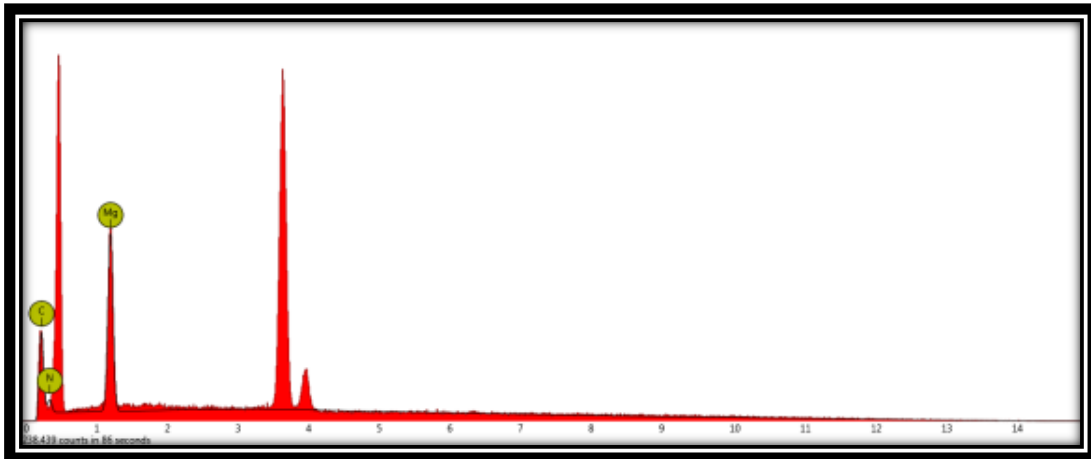


Figure 92: EDS graph of facies RU4 at square map

Table 30 Table of EDS analysis of facies RU4 at square map

Element Number	Element Symbol	Element Name	Confidence	Concentration	Error
12	Mg	Magnesium	100.0	51.2	0.8
6	C	Carbon	100.0	26.8	1.4
7	N	Nitrogen	100.0	22.0	4.5

Field Pictures

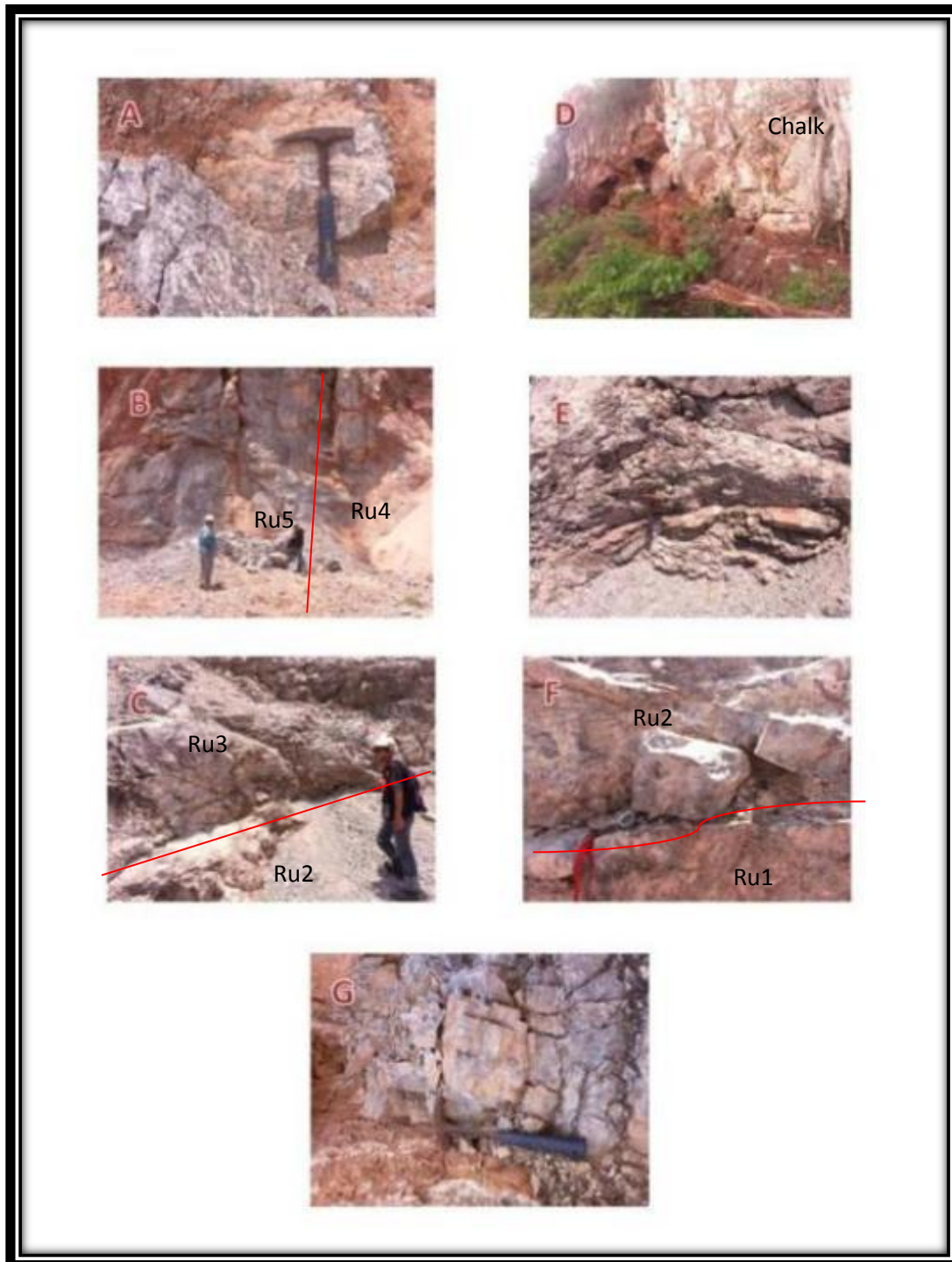


Figure 93: The picture of outcrops at quarry in Sungai Siput. (A) Facies Ru1 at the middle of two limestone hills. (B) Facies Ru4 and Ru5 contacts each others. (C) Facies Ru2 and Ru3 interbedded. (D) Facies Ru6 at the topmost hill and has chalk presented. (E) Facies Ru2 with highly jointed joint. (F) Facies Ru2 contacts with facies Ru1. (G) Facies Ru1 at the middle of two hills.



Figure 94: Photo of the hills and facies labels